Graphical Abstract

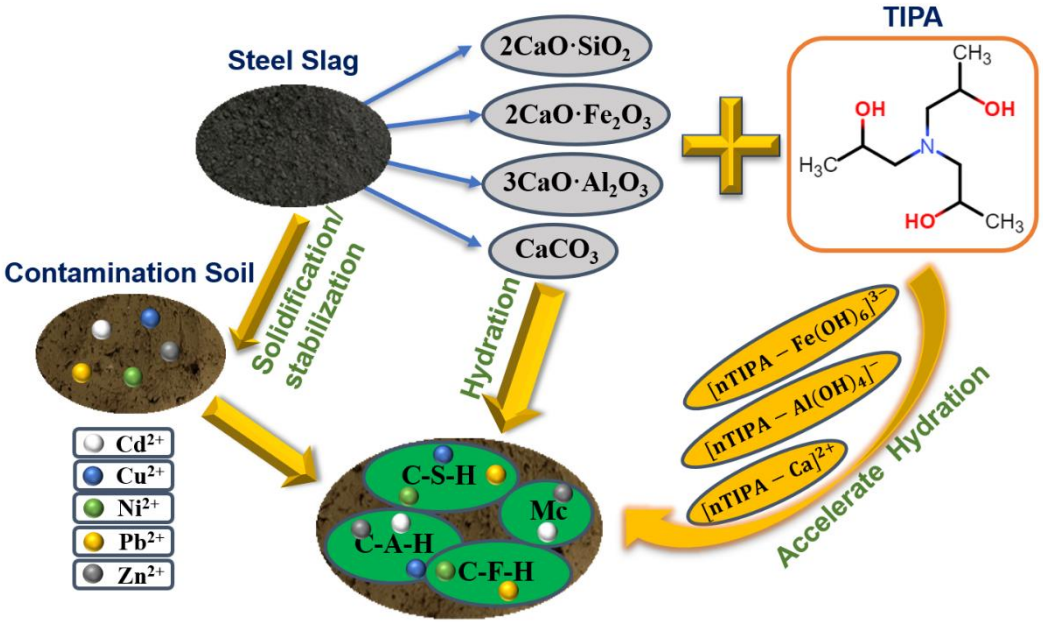

Highlights

- Alkanolamines promoted the hydration of steel slag and with TIPA showing the best performance.
- The UCS of treated HM-contaminated soil at 28 days was more than tripled using 0.1% TIPA-activated SS compared to the non-activated SS.
- TCLP leached concentrations of Cd, Cu, Ni, Pb, and Zn were reduced by 87.2%, 78.8%, 62.4%, 73.6% and 64.5% using 0.1% TIPA-activated SS at 28 days.
- Alkanolamines-activated SS is a sustainable alternative to PC in S/S for heavily-contaminated soil

Credit Author Statement

Bin Zeng: Conceptualization, Experiment, Writing - review & editing, Supervision, Project administration, Investigation.

Zhi Zhang: Methodology, Investigation, Data analysis, Writing - review & editing.

Shuo Yang: Data analysis, Writing review & editing.

Liwu Mo: Methodology, Data analysis, Writing - original draft, Writing - review & editing.

Fei Jin: Resources, Writing - review & editing, Supervision, Project administration, Investigation.

Declaration of Interest Statement

The authors declared that they have no conflicts of interest to this work. We declare that we do not have any commercial or associative interest that represents a conflict of interest in connection with the work submitted.

Alkanolamines-activated steel slag for stabilization/solidification of heavy metal contaminated soil

Bin Zeng[b], Zhi Zhang[b], Shuo Yang[b], Liwu Mo[a,b,*], Fei Jin[c]

[a] *State Key Laboratory of Materials-Oriented Chemical Engineering, Nanjing Tech University, Nanjing, Jiangsu 211800, PR China*

[b] *College of Materials Science and Engineering, Nanjing Tech University, Nanjing, Jiangsu 211800, PR China*

[c] *School of Engineering, Cardiff University, CF24 3AA, UK*

E-mail address: andymoliwu@njtech.edu.cn

Highlights:

- Alkanolamines promoted the hydration of steel slag and with TIPA showing the best performance.
- The UCS of treated HM-contaminated soil at 28 days was more than tripled using 0.1% TIPA-activated SS compared to the non-activated SS.
- TCLP leached concentrations of Cd, Cu, Ni, Pb, and Zn were reduced by 87.2%, 78.8%, 62.4%, 73.6% and 64.5% using 0.1% TIPA-activated SS at 28 days.
- Alkanolamines-activated SS is a sustainable alternative to PC in S/S for heavily-contaminated soil

Abbreviations:

SS: Steel slag **S/S**: Stabilization/Solidification **HM**: Heavy metals
TEA: Triethanolamine **TIPA**: Triisopropanolamine **EDIPA**: Ethyldiisopropylamine
DEIPA: Diethanolisopropanolamine **UCS**: Unconfined compressive strength
β-C_2S: β-larnite **$CaCO_3$**: Calcite **C_2F**: Srebrodolskite **$C_{12}A_7$**: Mayenite
C_3A: Tricalcium aluminate **C-S-H**: Calcium silicate hydrate **Mc**: Monocarboaluminate
CH: Portlandite **C-A-H**: Calcium aluminate hydrate **C-F-H**: Calcium ferrite hydrate
IC: Isothermal calorimetry **XRD**: X-ray diffraction **TGA**: Thermogravimetric analysis
TCLP: Toxicity Characteristic Leaching Procedure

Abstract: Steel slag (SS) is a byproduct discharged from steel-making industry with less than 25% utilization rate in China. The low utilisation rate of SS is associated with its low hydration activity in cement and concrete. In this study, four different alkanolamines (TEA, TIPA, EDIPA and DEIPA) were used to activate SS to improve its cementitious properties and metal binding performance, and hence its capacity on treating heavy metal-contaminated soils containing Cd, Cu, Ni, Pb and Zn.

Compared with the reference SS without activators, concentrations of leached Cd, Cu, Ni, Pb, and Zn have reduced by 87.2%, 78.8%, 62.4%, 73.6% and 64.5% by using 0.1% TIPA-activated SS after 28 days, and they were all below their respective regulatory limits by Standard for Pollution Control on the Hazardous Waste Landfill (GB 18598-2019) in China, and the unconfined compressive strength (UCS) of the treated soil at 28 days was enhanced by 237.7% using 0.1% TIPA-activated SS. To elucidate the activation mechanism, the hydration process of SS was thoroughly followed via isothermal calorimetry (IC) and conductivity analysis, and the nature of hydration products was studied by X-ray diffraction (XRD) and thermogravimetric analysis (TGA). It was concluded that alkanolamines facilitated the dissolution of minerals in SS and formation of hydration products (e.g., C-S-H, C-A-H, C-F-H and Mc), and hence significantly enhanced the microstructural development and engineering properties of SS. This work demonstrated a promising way of upcycling SS as an effective and sustainable S/S agent for handling complex heavy metal contaminated soil, with the potential of enhancing the SS utilization significantly.

Keywords: Alkanolamines, Steel slag activation, Heavy Metals, Soil Stabilization/Solidification

1. Introduction

Globally, heavy metals (HM) discharged from metal casting industries, fossil fuel burning, and the ever-growing use of gasoline, paint, chemical fertilizer and pesticide have been accumulating in soils in the past few decades[1]. Heavy metal-contaminated soil has become one of the most serious environmental issues all over the world, threatening human health [2-4]. A national soil survey found that in China 16.1% of the surveyed land exceeded national standards of soil contamination, within which 19.4% of agricultural land and 34.9% of former industrial land were regarded as contaminated [5-7], with HM as the most prevalent contaminants. HM such as cadmium (Cd), copper (Cu), nickel (Ni), lead (Pb), and zinc (Zn) are highly toxic [8, 9]. Effective and sustainable soil remediation technologies have been developed to treat HM-contaminated soil and achieved great successes in the past few years[10].

Stabilization/solidification (S/S) is the most widely-used technology in China to treat HM-contaminated soil (48.5% adoption rate in the 2017-2018 year) [11-13]. The method involves using binders to immobilize heavy metals in contaminated soil through physical encapsulation, adsorption and chemical reactions, which decrease the bioavailability/ecotoxicity of the contaminants and improve the engineering properties of the contaminated soils [14-16]. Previous studies had

highlighted the effectiveness of using highly alkaline cementitious materials in S/S, such as Portland cement (PC), MgO-based materials and lime-fly ash blends [17-19]. However, the production of these traditional binders was associated with intensive consumption of energy and nonrenewable resources, and contributed to ~10% of anthropogenic greenhouse gas emissions [20]. Furthermore, the high-alkaline binders may have adverse effects including incompatibility with HM, elevated soil pH and high HM leachability, particularly under aggressive environmental conditions [21-24], which limited the effectiveness of them in treating heavily-contaminated soils [25]. Therefore, it is always desirable to develop alternative binders with higher efficiency, better stability, low-cost and more environmentally friendly to remediate contaminated soils [12].

Steel slag (SS) is an alkaline industrial waste produced during the steelmaking process with an annual production of approximately 15-20 wt% of the total steel output worldwide [26, 27]. In China, the annual output of SS exceeded 100 million tons which accounted for approximately 24% of Chinese total industrial solid waste; nonetheless, its utilization rate is less than 25% [28]. Therefore, the large-scale utilization of SS is urgently needed as its disposal caused serious environmental pollution and occupied valuable lands [29]. Depending on the steelmaking method, the main chemical composition of SS is SiO_2, CaO, Al_2O_3, Fe_2O_3 and MgO. In terms of mineral forms, SS mainly consists of tricalcium silicate (C_3S), dicalcium silicate (C_2S), C_4AF, $C_{12}A_7$, C_2F, RO phase (metal oxides solid solution), free CaO and free MgO [30-33]. The composition of SS is similar to PC which shows its potential to be utilized as an alternative green binder in S/S for treating HM-contaminated soil. However, the hydration activity of SS is much lower than that of PC [34], which necessitates its activation prior to its application in S/S.

Alkali activation has been widely used to improve the hydraulic properties of SS using water glass, sodium hydroxide, sodium silicate and sodium sulfate, etc. [35, 36]. However, the production of those strong alkalis is not only associated with huge CO_2 emissions but also costly for large-scale SS utilization [37]. Additionally, owing to the ultra-high alkalinity of the alkali activators, the alkali-activated SS would also elevate the soil alkalinity and hence adversely impact the ecological balance of the environment. Therefore, developing a low-cost, environment friendly and effective activator for SS would pave the way for its application in HM-contaminated soil remediation.

Recently, it has been reported that alkanolamines could affect the structure of hydration products in

PC, and different types of alkanolamines exhibited different impacts [38-40]. Other researchers also found that alkanolamines could promote the hydration and chelating solubilization of SS [41, 42]. Thus, alkanolamines activated SS may serve as a promising alternative binder to remediate HM-contaminated soil considering: (i) the potential large-scale utilisation of SS which would reduce the negative environmental impact of SS accumulation; (ii) enhancement of the hydration of SS for improved S/S performance, particularly the early-age properties; (iii) the low cost and low carbon footprint of SS compared to PC. However, none has examined the performance of alkanolamines-activated SS for HM-contaminated soil remediation yet and there is a lack of understanding on the activation mechanism and optimal dosage of this new type of activator (i.e. alkanolamines) for SS. In this study, detailed analyses were conducted on the hydration kinetics, hydration products and strength of the hydrated SS by different alkanolamines including triethanolamine (TEA), triisopropanolamine (TIPA), ethyldiisopropylamine (EDIPA) and diethanolisopropanolamine (DEIPA) using characterization methods such as X-ray diffraction (XRD), isothermal calorimetry, thermogravimetric analysis (TGA) and Fourier transform infrared spectroscopy (FT-IR). The performance (i.e., strength and leachability of HM) of activated-SS treated HM-contaminated soils was assessed within 180 days to investigate the temporal effect of the type and dosage of the activators.

2. Materials and methods

2.1 Preparation of binders

The SS used in this study was derived from the Meishan Iron & Steel plant in China. Raw SS lumps were crushed, ball milled and then passed through a 20-mesh screen to obtain the SS powder, with its chemical compositions presented in Table 1. Both the concentrations of Cr and V ions in the TCLP leachates were below the detection limits indicating the low leachability of the two potential contaminants from the SS. The mineral components of the SS were examined by XRD (Fig. 1), which shows that the it mainly consists of β-larnite (β-C_2S), Calcite ($CaCO_3$), srebrodolskite (C_2F), mayenite ($C_{12}A_7$), tricalcium aluminate (C_3A).

Fig. 2 shows the chemical structures of the four types of alkanolamines (AR grade) used in this work, of which the TEA and TIPA were provided by Aladdin corporation, and EDIPA and DEIPA were provided by Hongbaoli Co., Ltd. The activators were combined with SS powders according to

the proportions in Table 2 and then milled in a planetary ball mill at a speed of 220 r/min for 30 min to obtain the activated SS.

Table 1

Chemical compositions of SS measured by XRF.

Chemical composition (wt%)	CaO	Fe_2O_3	SiO_2	Al_2O_3	MgO	MnO	P_2O_5	TiO_2	Cr_2O_3	V_2O_5	LOI
Steel slag	35.89	25.49	14.77	8.23	6.30	3.55	2.32	0.97	0.24	0.21	1.12

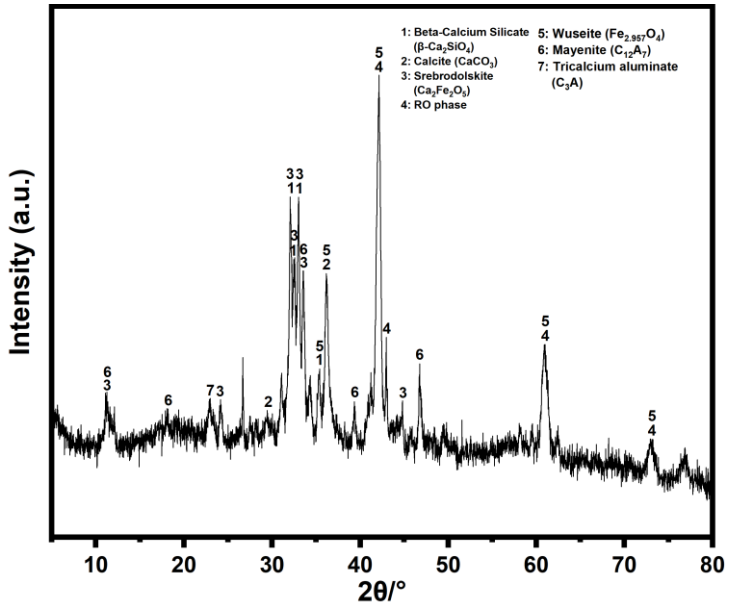

Fig. 1 XRD pattern of SS

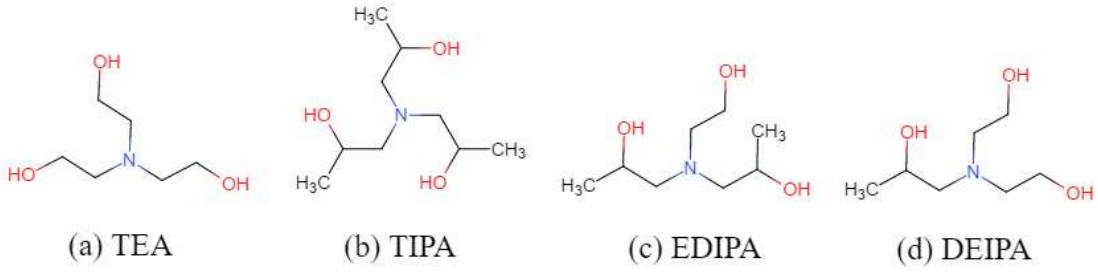

Fig. 2 Schematic representation of the molecular structures of the four alkanolamines used in this study

Table 2

The type and content (by weight of SS) of alkanolamines used as activators

	Alkanolamines	Content (%)
Control	None	-
TIPA-0.02	TIPA	0.02
TIPA-0.05	TIPA	0.05
TIPA-0.08	TIPA	0.08
TIPA-0.1	TIPA	0.1
TEA-0.05	TEA	0.05

EDIPA-0.05	EDIPA	0.05
DEIPA-0.05	DEIPA	0.05

2.2 Mechanistic study on the activation of SS by alkanolamines

2.2.1 Compressive strength tests of activated SS paste

The SS pastes activated by alkanolamines with water to solid ratio of 0.2 were prepared and cast in 20 mm × 20 mm × 20 mm moulds. These samples were cured in a moist cabinet under the condition of 20 ± 1 ℃, 95 ± 1% relative humidity for 24h, and then demoulded and placed in the isothermal curing cabinet under the same condition until the testing age (1d, 3d, 7d, 28d, 90d and 180d). The mean compressive strength of six cement pastes was recorded for each mix. The crushed samples were ground, sieved and then immersed in ethanol for terminating hydration, followed by drying at 60°C for 24 h in a vacuum oven until further characterization.

2.2.2 Isothermal calorimetry

The hydration heat of activated SS was measured by a Thermometric TAM Air isothermal calorimeter (TA Instruments) at 20 ± 0.02 ℃. Approximately 4 g of dry powders were loaded in glass ampoules, and syringes were loaded with 2 g of water. When a steady baseline was reached, the solution was injected into glass ampoules and externally stirred for 20 s. Then the glass ampoule was sealed and placed into the isothermal calorimeter. The heat of hydration was measured for 3 days to study the effect of activator on the hydration of SS.

2.2.3 Liquid phase conductivity

The dissolution rates of the reference and activated SS were followed by measuring the conductivities of the SS slurries. The slurries were prepared by mixing the SS and water with a liquid/solid ratio of 5. The magnetic stirrer was used for the mixing process at 250 rpm and stirred for 48h. The conductivities of the slurries were continuously recorded by a conductivity meter (DDSJ-308A, made in Shanghai Yueping).

2.2.4 X-ray diffraction (XRD)

XRD analysis was conducted on D/max-2500 X-ray diffraction of Rigaku, Japan, with CuKα radiation, 40 kV voltage, 200 mA current, 2θ between 5°and 80°, 0.02°/s scan speed and 0.02° step size to characterize the mineralogical phases of SS at different ages.

2.2.5 Thermogravimetry/differential scanning calorimetry (TG-DTG)

Thermogravimetric and differential thermogravimetric analysis (TG/DTG) was operated under N_2

161 flow with heating rate of 10℃/min from the ambient temperature to 1000℃ using STA409C
162 instrument of NETZSCH.

163 *2.3 Preparation of contaminated soils*

164 A clean soil was obtained by sampling a surface soil up to 50 cm depth from Xinxiang of Henan
165 Province, China, and dried in an oven at 105℃ for 6 hours. The dried soil was crushed, ground and
166 then passed through a 1 mm sieve and stored in a polyethylene container for the subsequent
167 physicochemical properties tests and the results were shown in Table 3. HMs were not leached from
168 clean soil and SS used in the experiments by the TCLP method. In this work, a heavily HM-
169 contaminated soil was prepared via doping Cd, Cu, Ni, Pb and Zn (in the form of $Cd(NO_3)_2{\cdot}4H_2O$,
170 $Cu(NO_3)_2 \cdot 3H_2O$, $Ni(NO_3)_2 \cdot 6H_2O$, $Pb(NO_3)_2$, $Zn(NO_3)_2 \cdot 6H_2O$ respectively, AR grade from
171 Sinopharm Chemical Reagent Co., Ltd.) to the clean soil. Predetermined amounts of HM (i.e., 24
172 mg/kg of Cd, 10000 mg/kg of Cu, 500 mg/kg of Ni, 280 mg/kg of Pb and 12500 mg/kg of Zn by
173 weight of dry soils) were firstly dissolved into the solution and added to the dry soil (to keep the
174 moisture content at 20%) and then stirred vigorously for 30 min to prepare the co-contaminated soil.
175 The mixture was sealed and kept for 24 hours to ensure the adequate distribution of HM in soil. The
176 binder and water were then added and mixed to achieve homogeneity. The weight ratio of binder to
177 soil is 2:8 and the final weight ratio of water to solid (including soil and binder) was determined as
178 25:100 since preliminary results showed that consistencies of the mixtures were optimal at this level
179 (i.e., neither too dry nor too wet for handling). After that, approximately 200 g of the mixture was
180 statically compacted by a stainless steel cylindrical mold with 50 mm diameter and 50 mm height.
181 Then, the specimen was carefully extruded from the mold using a hydraulic jack and sealed in a
182 polyethylene bag for curing under the standard condition (temperature 20 ± 2 ℃, relative humidity
183 99%). Specimens were collected for various tests at ages of 1, 3, 7, 28, 90 and 180 days.

184 **Table 3**

185 Basic physicochemical properties of the soil

Property	Value[b]	Test method
Specific gravity, G_s	2.59	ASTM D854-14
Liquid limit, w_L (%)	33.4	ASTM D4318-10
Plastic limit, w_P (%)	17.2	ASTM D4318-10
Optimum water content, w_{opt} (%)	21.8	ASTM D698-12

Maximum dry density, ρ_d (g/cm^3)	1.82	ASTM D698-12
Average soil pH	8.19	ASTM D4972-13
Soil classification	CL	ASTM D2487-11
Grain size distribution (%)[a]		-
Clay (<0.002 mm)	22.5	
Silt (0.002–0.075 mm)	51.7	
Sand (0.075–2 mm)	25.8	

[a] Measured using a laser particle size analyzer Mastersizer 2000 (Malvern, USA).

[b] Number of replicate = 3, and coefficient of variance (COV) < 5%.

2.4 Unconfined compressive strength (UCS) tests for contaminated soils

The microcomputer-controlled electronic universal testing machine of Shanghai Yihuan Instrument Technology Co., Ltd was used to assess the UCS of contaminated soils according to JTG E51-2009[43], at a speed of 1 mm·min^{-1}. The mean UCS of six soil samples was recorded for each mix and presented here. The crushed samples were collected, ground and sieved through a 4 mm mesh before leaching tests.

2.5 Leaching test for contaminated soils

After incubation for designated time periods, specimens were firstly dried at 65 ℃ to achieve constant weights. The leachabilities of Cd, Cu, Ni, Pb and Zn in the samples was evaluated according to US EPA Method 1311 - Toxicity Characteristic Leaching Procedure (TCLP). Briefly, approximately 5 g of the crushed sample was added to ~96.5 mL deionized water and stirred for 5 min and the pH value (which determines buffer solution chose) of the mixture was recoded with a pH meter (Rex PHS-3E). The soil and buffer solution (HOAc/NaOAc, pH 4.93) were mixed with a solid/liquid ratio of 1:20 in a 2 L polyethylene bottle and shaken at 250 rpm for 18 h. Cd, Cu, Ni, Pb and Zn concentrations in the filtrates were measured by ICP-OES after filtration with 0.45μm filter, dilution (if necessary) and acidification to pH < 2.

2.6 Statistical analysis

All compressive strength experiments were carried out in sextuplicate, and leaching experiments were carried out in triplicate. The mean and standard deviations of each experiment were presented. The significance of differences between groups was determined by one-way ANOVA using Duncan method with a significance level of 0.05 using SPSS 17, and indicated by different lowercase letters in the figures.

3. Results

3.1 Hydration properties of alkanolamine-activated SS

As the capacity to solidify and stabilize HM was closely related to the binder's hydration characteristics, the following sections will focus on the hydration mechanisms and evolution of mineral compositions of the alkanolamine-activated SS.

3.1.1 Heat evolution

The reaction of SS with water was a thermodynamic reaction accompanied by exothermic behavior, which could be recorded using conduction calorimetry. The heat release curves were characterized by the presence of two peaks. The initial peak was attributed to the dissolution of f-CaO, C_3A and $C_{12}A_7$ [44, 45], leading to the continuous accumulation of ions. When the ion concentrations reached a certain level, the second exothermic peak appeared, ascribed to the precipitation of the CH (portlandite) and C-S-H (calcium silicate hydrate) phases [46] and the dissolution of β-C_2S and C_2F [47]. The hydration process gradually stabilized after the second exothermic peak.

Fig. 3 shows the effect of different alkanolamines on the hydration heat evolution rate and cumulative hydration heat of SS. All the alkanolamines increased the heat generation significantly. No significant difference was observed for the appearance time of the first exothermic peak, while the second peak appeared the earliest for TEA and latest for TIPA. The second peak was not observed for the control sample, which is likely due to the low hydration reactivity of the SS used in this work and hence the 2nd peak may appear beyond 72 hours.

Fig. 4 presents the effect of TIPA dosage on the hydration heat evolution rate and cumulative hydration heat. The first peak increased significantly with the increased TIPA content indicated that a higher dosage of TIPA improved the dissolution of mineral phases. Moreover, higher TIPA dosage shortened the induction period for the second peak, implying that time had reduced for the ion concentrations to reach supersaturation with the addition of more TIPA. The cumulative hydration heat increased proportionally with the dosage of TIPA.

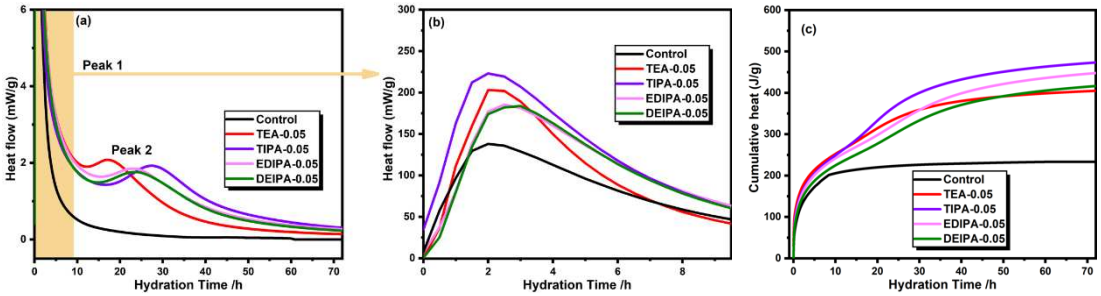

Fig. 3 Hydration heat evolution of different alkanolamines-activated SS: (a) Heat flow of the whole hydration process, (b) heat flow in the first 9 h (Peak 1) and (c) cumulative hydration heat.

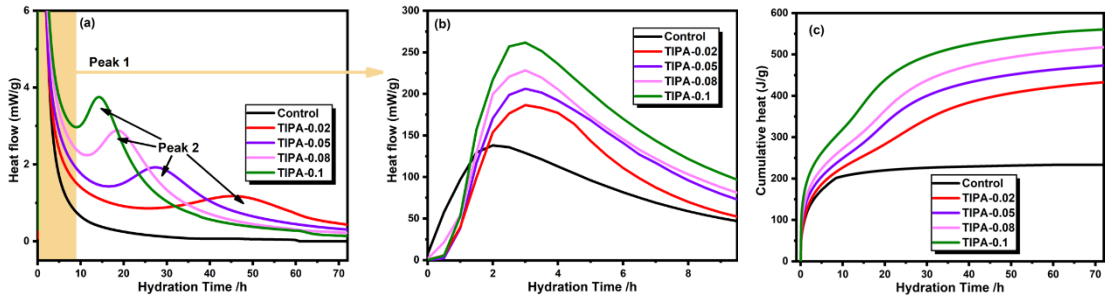

Fig. 4 Hydration heat evolution of TIPA-activated SS at different TIPA dosages: (a) Heat flow of the whole hydration process, (b) heat flow in the first 9 h (Peak 1) and (c) cumulative hydration heat.

3.1.2 Conductivity of SS slurries

The ion concentrations in the aqueous phase could be indirectly assessed by measuring the conductivity of the solution, which could be used to evaluate the dissolution rate of SS [48]. Fig. 5 shows the evolution of conductivity in the SS slurries with and without alkanolamines. The conductivity reached the peak at the first 5 min due to the dissolution of the high solubility mineral phases (e.g., free lime and aluminates). This was followed by the ionic reactions in the solution leading to rapidly decreased conductivity. After approximately 60 min, the conductivities of the SS solutions with activators rose again and then dropped gradually over time, while this second peak was not observed in the control sample. Apparently, the activators promoted the dissolution of SS again when the ion concentration dropped, which induced the second peak.

For the control sample, the precipitation of the hydration products continuously consumed the dissolved ions. Meanwhile, the dissolved cations adsorbed on the surface of SS particles and formed a coating layer, which was not conducive to further dissolution [49]. This explains the gradually decreased conductivity and higher residual conductivity over time due to the diffusion-controlled dissolution of SS particles over time, ascribed to the surface coating. With the addition of alkanolamines, the chelating of cations led to exposed SS surface for further dissolution, which was evidenced by the second peak. Moreover, chelation likely resulted in higher supersaturation degrees of the ions in the solution, which induced more hydration/precipitation products. This is the reason of the much lower residual conductivities of the SS samples with activators. Among the four alkanolamines, TIPA showed the highest second peak and lowest residual conductivity, indicating

its best performance as the chelating agent for promoting the hydration of SS. Fig. 5 (b) shows that the effect of TIPA is highly correlated with its dosage. Increasing the dosage from 0.02% to 0.1% proportionally increased the conductivity of the second peak and reduced the residual conductivity of the solution.

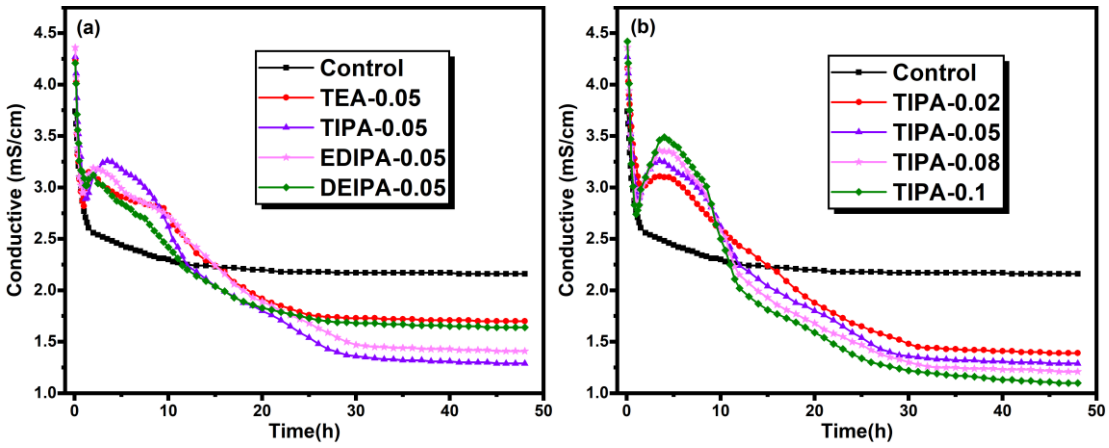

Fig. 5 Evolution of conductivity in the SS solutions with and without alkanolamines: (a) SS with four different alkanolamines at the same dosage of 0.05%, (b) SS with 0.02%, 0.05%, 0.08% and 0.1% TIPA.

3.1.3 XRD

The hydration products were characterized by XRD in Fig. 6. Compared with unhydrated SS (Fig. 1), the peaks of C_3A disappeared and the peaks of β-C_2S, C_2F, $C_{12}A_7$ and $CaCO_3$ weakened. Moreover, the peaks of hydration products such as $Ca_3Fe_2Si_{1.15}O_{4.6}(OH)_{7.4}$, $Ca_3Al_2(O_4H_4)_3$ and $C_4(A,F)\check{C}H_{11}$ appeared, which could be formed by the hydration of C_3A, $C_{12}A_7$, C_2F and $CaCO_3$. Moreover, hydration of β-C_2S would form C-S-H and these hydration products would potentially contribute to the cementitious and metal-binding capability in soil S/S. As shown in Fig. 6 (a), the peaks of hydration products of activated SS were stronger than those of SS without activators. The enlarge view ($2\boldsymbol{\theta}$ = 31.5°-34.0°) clearly exhibits that the characteristic peaks of β-C_2S and C_2F weakened further after the addition of activators, indicating higher dissolution/reaction rates of these mineral phases. Consistent with the conductivity results, SS activated by TIPA exhibited the lowest peaks of β-C_2S, C_2F and highest peaks of the hydration products compared with other activators. Fig. 6 (b) further demonstrated that the dissolution of the minerals in SS and the precipitation of the hydration products were promoted by the increased dosage of TIPA from 0.02% to 0.1%.

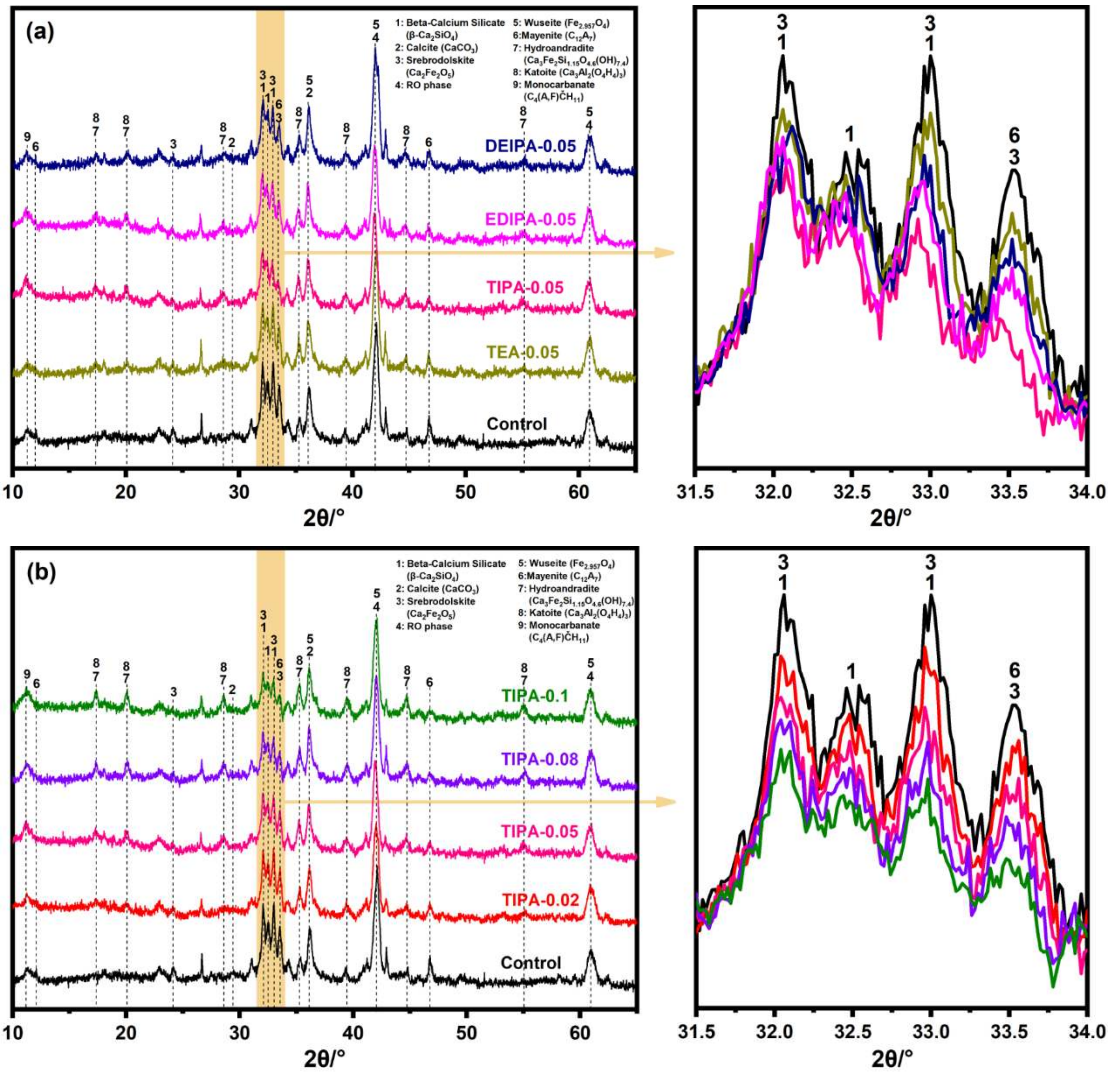

282

283

284 **Fig. 6** XRD patterns of phase compositions in hardened SS pastes at 28 days activated by: (a) four different

285 alkanolamines, (b) 0.02%, 0.05%, 0.08% and 0.1% TIPA.

286 *3.1.4 Thermogravimetric analysis (TGA)*

287 During SS hydration, mineral phases reacted with water to form hydration products, and hydration

288 products were readily carbonated to form corresponding carbonates. In order to investigate the

289 effects of activator type and dosage on the hydration of SS, the hydration products of SS paste were

290 characterized by TGA as shown in Fig. 7. It could be seen from the derivative thermogravimetric

291 (DTG) curve that there were mainly three mass loss peaks. The peak at ~140 ℃is mainly due to the

292 dehydration of C-S-H gel and Mc (monocarboaluminate). The peak at ~280 ℃is mainly ascribed to

293 the dehydration of C-A-H (calcium aluminate hydrate) and C-F-H (calcium ferrite hydrate) [29, 50].

294 In the range of 650-750 ℃, the peak is mainly due to the decarbonation of $CaCO_3$ [51]. C-S-H gel

295 was generated from the hydration of silicate phases, C-A-H and Mc from aluminates, and C-F-H

from C_2F. Moreover, a portion of $CaCO_3$ was reacted and produced Mc.

Fig. 7(a) showed the TG and DTG curves of the SS pastes at the age of 28 days activated by the four alkanolamines. Compared with the control sample, the first two peaks were much more pronounced in the samples with activators, while the one associated with $CaCO_3$ was weaker. Moreover, TIPA-activated SS showed the maximum weight losses due to C-S-H, Mc, C-A-H and C-F-H decomposition and the minimum weight loss of $CaCO_3$ decomposition. In Fig. 7(b), higher dosage of TIPA increased the peaks associated with hydration products while decreased the one with $CaCO_3$. The TGA results agreed well with other tests on the best activation performance of TIPA and the enhanced effect by increasing its dosage.

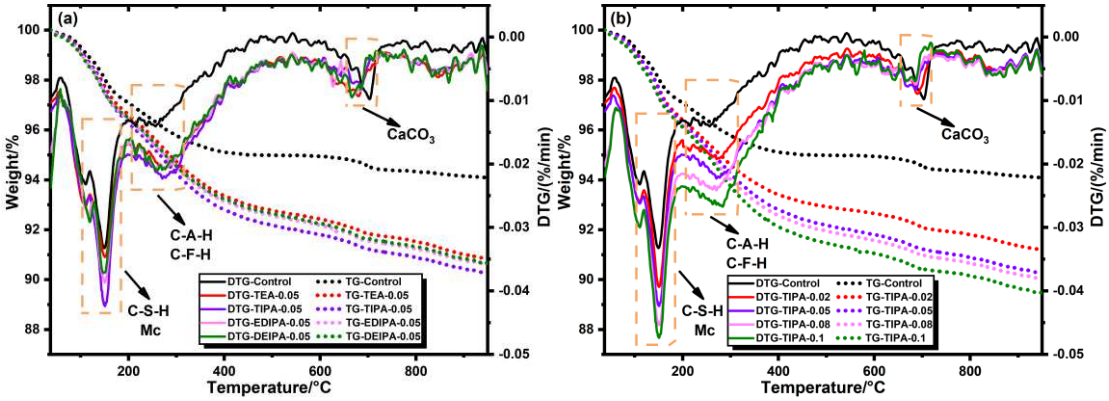

Fig. 7 TG-DTG curves of hardened SS pastes at 28d activated by: (a) four different alkanolamines at the same addition dosage of 0.05%, (b) 0.02%, 0.05%, 0.08% and 0.1% TIPA.

3.2 Compressive strength of alkanolamine-activated SS pastes

The effects of four different alkanolamines on the mechanical properties of hardened SS pastes were evaluated by measuring the compressive strength of SS pastes at different ages as shown in Fig. 8(a). It could be seen that the compressive strength gradually increased with curing time with the rate decreased. Moreover, the activators significantly improved the compressive strength of the hardened SS pastes with the effectiveness decreasing in the order of TIPA>EDIPA>DEIPA>TEA. Specifically, at 28d, the compressive strength of the SS paste without activators was only 14.8 MPa, which was increased to 27.1, 34.6, 30.9 and 28.6 MPa after adding 0.05 % TEA, TIPA, EDIPA and DEIPA, respectively. Fig. 8(b) showed the effect of TIPA dosage on the compressive strength, demonstrating the positive correlation between TIPA dosage and the improvement of compressive strength, agreeing well with the increased quantities of hydration products. It is worth noting that adding only 0.1% of TIPA to SS enhanced the compressive strength by ~190% and ~140% at 28d

and 180d, respectively.

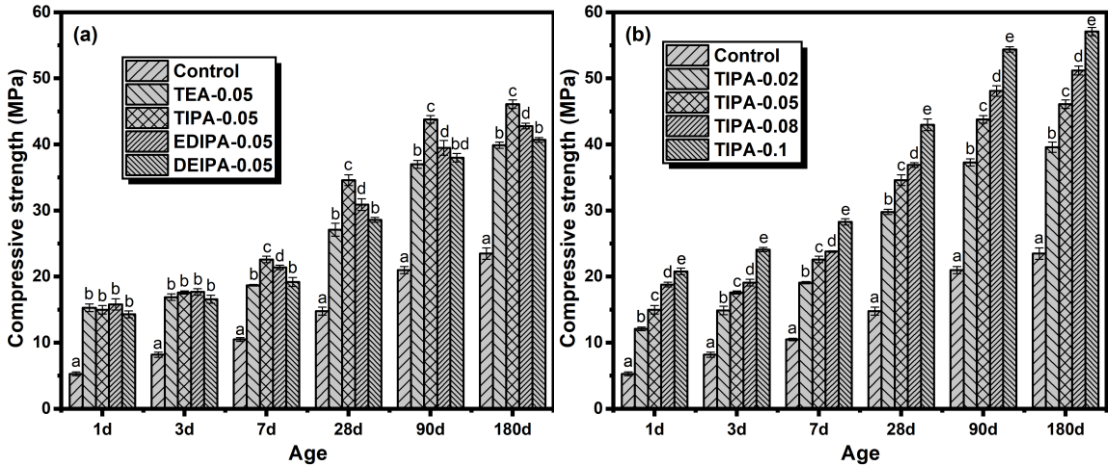

Fig. 8 Effect of activators on compressive strength of activated SS pastes: (a) four alkanolamines (TEA, TIPA, EDIPA and DEIPA) at the same dosage of 0.05% and (b) 0.02%, 0.05%, 0.08% and 0.1% TIPA.

3.3 UCS of activated-SS treated HM-contaminated soil

The UCS test has been widely used to describe the mechanical properties of S/S soils. The type of binder and curing age have significant impacts on the physicochemical properties of the HM-contaminated soil treated with S/S. In general, the development of UCS of treated soils was consistent with the results of the paste samples (comparing Fig.9 and Fig. 8). All the activators showed excellent performance in the presence of high concentrations of multiple HMs in the soils. TIPA-activated SS exhibited the highest strength among all the alkanolamines (Fig. 9a) and its effect on UCS was positively correlated with the dosage (Fig. 9b). The UCS results demonstrated that by adding as low as 0.02% of TIPA to SS, the strength could be improved by more than 100% at all ages, which showed their excellent compatibility with HMs and great promise to reduce the use of SS usage in contaminated soil S/S.

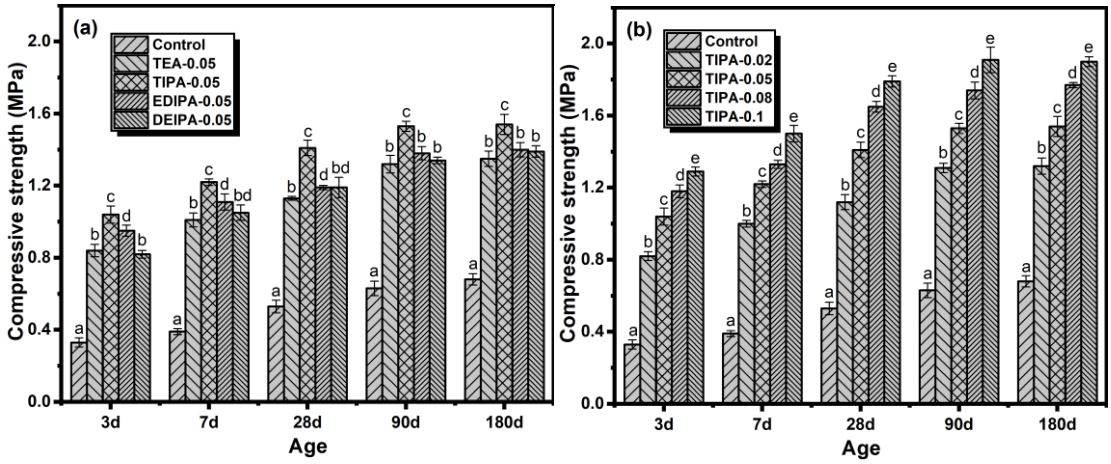

Fig. 9 Effect of activated-SS on the UCS of HM-contaminated soil: (a) four alkanolamines (TEA, TIPA, EDIPA and DEIPA) at the same dosage of 0.05% and (b) 0.02%, 0.05%, 0.08% and 0.1% TIPA.

3.4 TCLP results of activated-SS treated HM-contaminated soil

3.4.1 Effect of different alkanolamines

The concentrations of leached HM, i.e., Cd, Cu, Ni, Pb and Zn in contaminated soils treated by alkanolamine-activated SS were shown in Fig. 10. Apparently, the leachability of all the HM were significantly reduced after S/S over time, which indicated that SS exhibited superior capacity in solidifying and stabilizing the HM in the contaminated soil. With activators, the effectiveness of HM stabilization was improved, while the type of activator did not seem to influence the early-age leachability of HM significantly up to 7 days. Above 28 days, TIPA and EDIPA showed the best performance among all the alkanolamines for the TCLP results. Moreover, it is worth noting that 0.5% of TIPA successfully lowered the leached concentrations of all the HM (except for Ni, which barely exceeded the limit) to below their regulatory limits (see Standard for Pollution Control on the Hazardous Waste Landfill (GB 18598-2019) [52]) in China after curing of 28 days.

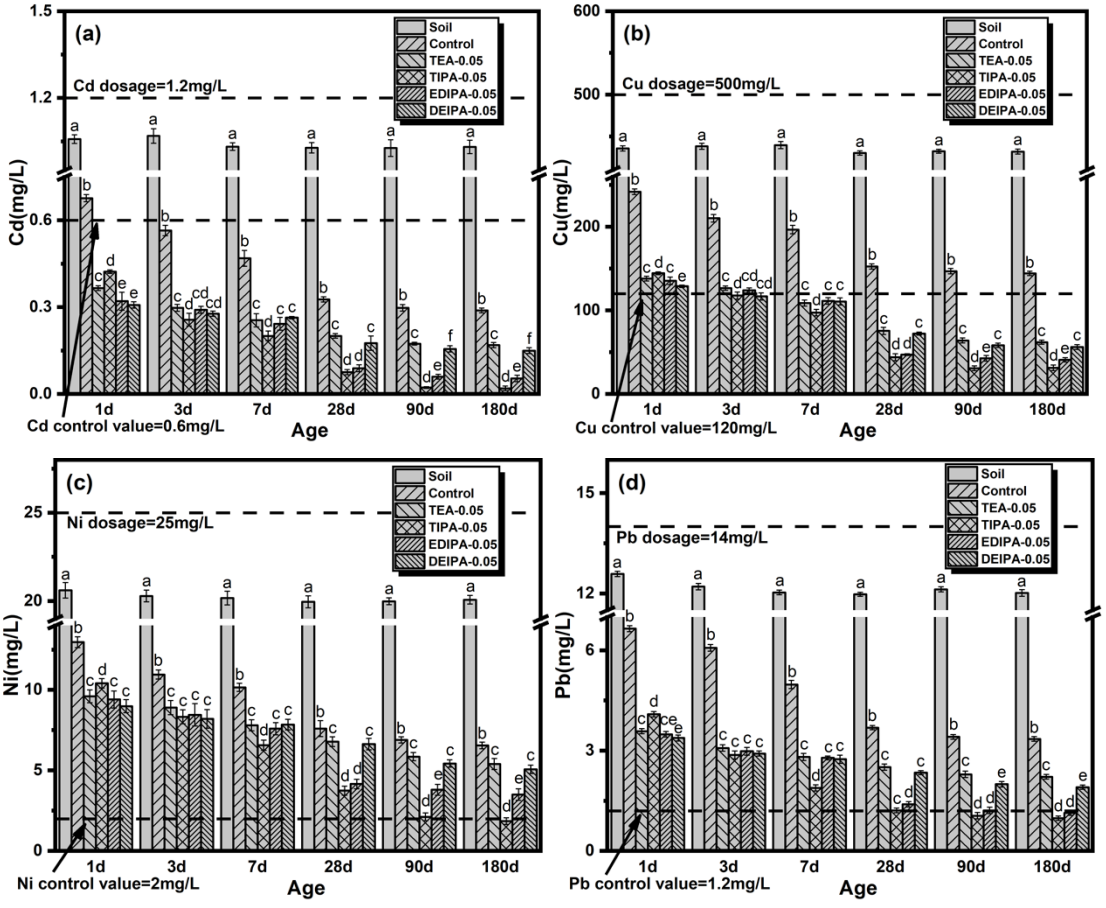

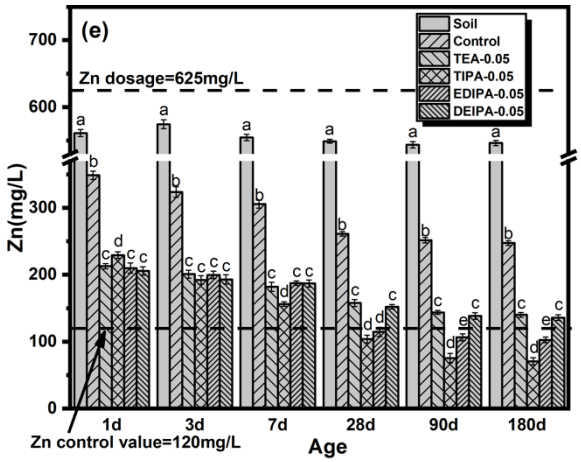

Fig. 10 Effect of different alkanolamines (TEA, TIPA, EDIPA and DEIPA at 0.05% dosage) activated SS on the leachability of HM: (a) Cd, (b) Cu, (c) Ni, (d) Pb and (e) Zn.

3.4.2 Effect of TIPA dosage

According to the above results, TIPA showed the highest effectiveness to solidify and stabilize HM in contaminated soil. Thus, the effect of its dosage on the leachability of HM was investigated with TCLP results shown in Fig. 11. All the HM showed decreased leached concentrations over time. Consistent with the hydration and mechanical results, more TIPA showed improved HM immobilization capacity due to the enhanced hydration of SS. At the dosage > 0.8% the leachability of Ni also dropped to below its regulatory limit at 90 days.

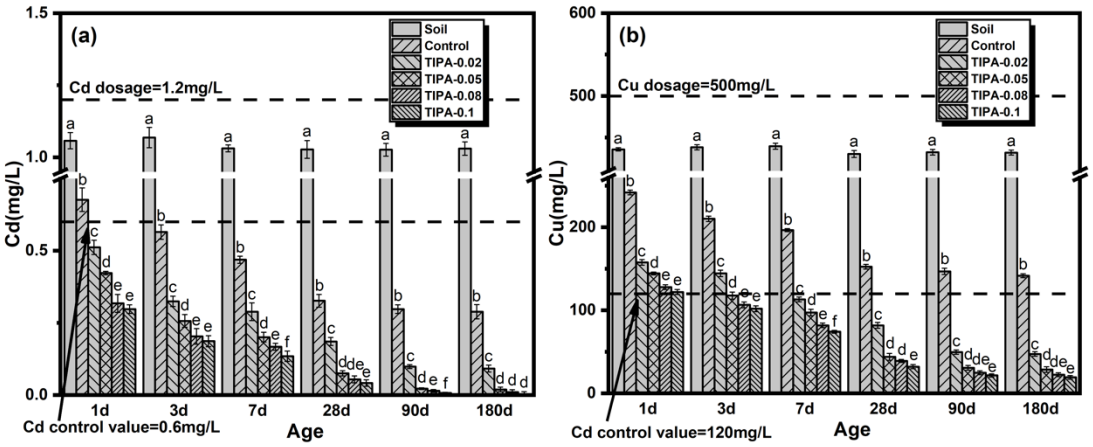

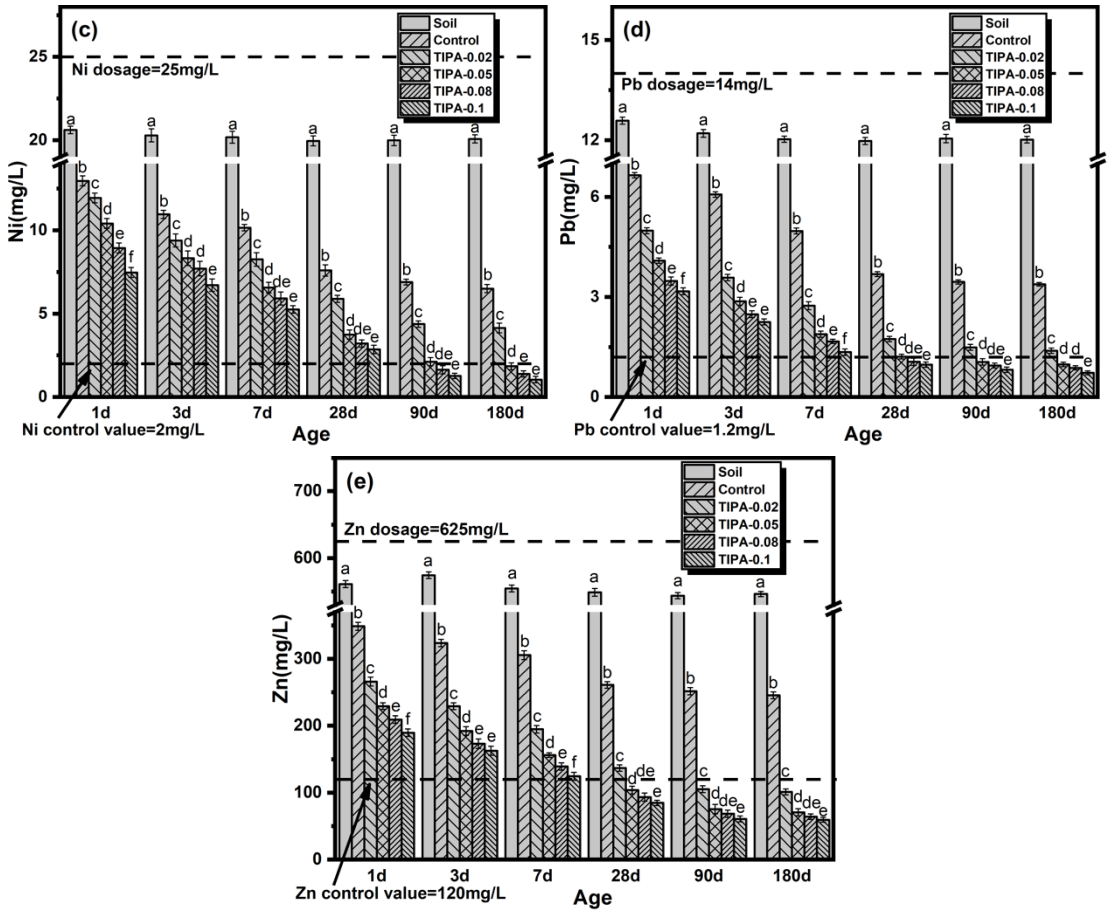

Fig. 11 Effect of dosage of TIPA (0.02%, 0.05%, 0.08% and 0.1%) activated SS on the leachability of HM: (a) Cd, (b) Cu, (c) Ni, (d) Pb and (e) Zn.

4. Discussion

Based on the experimental results presented above, TIPA was found to be the best activator among the four types of alkanolamines, which was studied in detail. Hence the following sections will use TIPA as the representative alkanolamine to elucidate its effect on SS hydration and soil S/S performance.

4.1 Effect on the hydration process

The hydration process of TIPA-activated SS was characterized by the evolution of hydration heat and conductivity over time, and the results agreed well (see Figs. 4 & 5). The hydration process is hence divided into two stages. The first stage is the continuous dissolution of minerals and gradual accumulation of ions in the pore solution. TIPA effectively promotes the dissolution of SS, which was evidenced by the enhancement of the first exothermic peak of hydration heat and the first conductivity peak. This effect is more pronounced with the increased dosage of TIPA. Moreover, the dormant periods between the first and second peak (not observed in the reference SS samples

within the test time) in both the heat and conductivity evolution curves were significantly reduced, indicating the fast accumulation of ions to achieve the supersaturations for hydration products, which induced the second stage. The second stage is the precipitation of hydration products. The enhancement of second peak of hydration heat and the increased difference between the peak and residual conductivity showed that TIPA led to the formation of more hydration products. Similarly, this effect is positively correlated with the dosage of TIPA. This was further evidence by the XRD and TGA results. Hence, the strength of the SS pastes improved remarkably with the increase of TIPA content (Fig. 8).

4.2 Effect on the hydration products

As shown in the XRD and TGA (see Figs. 6 &7), TIPA promoted the dissolution of minerals in SS and the formation of hydration products. This effect is mainly exerted in two ways. The first one is the promotion of the hydration of C_2S, aluminates and C_2F, resulting in the formation of C-S-H, C-A-H and C-F-H. The other way is the enhanced reaction between C-A-H, C-F-H and $CaCO_3$, thereby producing a large amount of Mc.

The mineral phases in SS first dissolve into ions, which accumulate in the cement pore solution (Equations 1-3), and they react with each other to form hydration products. The alkanolamines chelated with the metal ions, which increased the solubility of the minerals and the concentrations of ions [29, 42].

$$2(2CaO \cdot SiO_2) + 4H_2O \rightarrow 3CaO \cdot 2SiO_2 \cdot 3H_2O + Ca^{2+} + 2OH^- \quad (1)$$

$$3CaO \cdot Al_2O_3 + 6H_2O \rightarrow 3Ca^{2+} + 2Al(OH)_4^- + 4OH^- \quad (2)$$

$$2CaO \cdot Fe_2O_3 + H_2O + 2OH^- \rightarrow 2Ca^{2+} + 2Fe(OH)_6^{3-} \quad (3)$$

The ions in the pore solution were chelated by TIPA and would not immediately participate in the precipitation reaction. According to Le Chatelier's principle, the forward progress of reactions (1)-(3) were facilitated until a new value of the dissolution equilibrium constant K was reached [53]. Thus, TIPA promoted the dissolution of mineral phases and increased the amount of various dissolved metal ions in the solution. The precipitation reactions of ions are described in Equations (4) - (8).

$$3Ca^{2+} + 2Al(OH)_4^- + 4OH^- \rightarrow 3CaO \cdot Al_2O_3 \cdot 6H_2O \quad (4)$$

$$3Ca^{2+} + 2Fe(OH)_6^{3-} \rightarrow 3CaO \cdot Fe_2O_3 \cdot 6H_2O \quad (5)$$

$$3Ca^{2+} + 2Al(OH)_4^- + CaCO_3 + 4OH^- + 5H_2O \rightarrow 3CaO \cdot Al_2O_3 \cdot CaCO_3 \cdot 11H_2O \quad (6)$$

$$3Ca^{2+} + 2Fe(OH)_6^{3-} + CaCO_3 + 5H_2O \rightarrow 3CaO \cdot Fe_2O_3 \cdot CaCO_3 \cdot 11H_2O \quad (7)$$

$$4Ca^{2+} + (2x)Al(OH)_4^- + [2(1\text{-}x)]\, Fe(OH)_6^{3-} + CO_3^{2-} + 4xOH^- + 5H_2O$$

$$\rightarrow\ 3CaO \cdot xAl_2O_3 \cdot (1-x)Fe_2O_3 \cdot CaCO_3 \cdot 11H_2O \quad (8)$$

The precipitation led to the reduction of metal ion concentrations in the pore solution, resulting in the release of ions from their chelated forms, further promoting the precipitation of more hydration products. The dissolution and precipitation reactions are hence both promoted by TIPA which acts like a "catalyst" in the process. In summary, TIPA promoted the dissolution of mineral phases such as C_2S, C_3A, $C_{12}A_7$, and C_2F, thereby increased the amount of metal ions in the solution, and hence promoted the subsequent precipitation reaction of generating C-S-H, C-A-H, C-F-H and Mc. Nevertheless, how different alkanolamines interacted with the ions and affected the hydration of SS differently remain unclear.

4.3 Effect on the S/S performance for HM-contaminated soil

TIPA-activated SS showed excellent compatibility with the heavily contaminated soil, which was evidenced by the UCS of the mixtures (see Fig.9). Moreover, the leachability of all HM (except for Ni) can be successfully reduced to below their regulatory limits with only 0.5% of TIPA in SS at the curing age of 28 days, while Ni was successfully treated at 90 days with 0.8% TIPA-activated SS. The outstanding S/S performance is partly due to the enhanced solidification due to better cementitious properties of TIPA-activated SS and also due to the enhanced chemical stabilisation of HM in the hydration products such as C-S-H, C-A-H, C-F-H and Mc [54-56]. Moreover, TIPA may also play a role in stabilizing HM by chelation, which warrant further studies. Leaching effect of HM in the hydration products of alkanolamines activated SS was shown in Fig. S1 and Fig. S2. The leaching of each heavy metal remained relatively constant after the age of 28d, which demonstrates that the solidification and stabilization of heavy metals by SS hydration products is firm and stable. This study demonstrated that alkanolamines could improve the capacity of SS to solidify and stabilize HM-contaminated soil. Firstly, it provides a sustainable alternative to Portland cement in S/S to reduce energy consumption and carbon emission in cement production. Secondly, it will

enhance the utilization of SS to reduce the environmental impact and waste of land resources. However, there are many challenges and opportunities to apply this novel binder in the field which include but not limited to: (i) optimisation of the alkanolamines/SS and SS/soil ratios depending on the type, concentration of the contaminants and the soil type; (ii) long-term performance of the treated soils under different climatic conditions; and (iii) variability of the SS composition in the world and hence the potential of leaching inherent contaminants in SS in the long term.

5. Conclusion

Four types of alkanolamines (TEA, TIPA, EDIPA and DEIPA) were used to activate SS and then remediate HM-contaminated soil. The effects of alkanolamines on the hydration process and hydration products of SS were thoroughly investigated via a series of techniques. Moreover, their effects on the stabilization/solidification performance of HM-contaminated soil were assessed via strength and leaching tests. The following conclusions could be drawn:

1. The addition of alkanolamines promoted the hydration process of SS and hence facilitated the formation of hydration products. The chelation of dissolved metal ions promoted the dissolution of mineral phases in SS and the subsequent precipitation reaction. The hydration products such as C-S-H, C-A-H, C-F-H and Mc were beneficial to solidify and stabilize heavy metal contaminated soil.

2. TIPA showed the best activation effect among all the investigated alkanolamines and better promotion effect could be obtained with higher dosage. Compared to the reference SS paste, the compressive strength of the 0.1% TIPA-activated SS was enhanced by 190.5% at 28 days.

3. TIPA-activated SS showed excellent performance in HM-contaminated soil stabilization/solidification. Leached concentrations of Cd, Cu, Ni, Pb, and Zn have reduced by 87.2%, 78.8%, 62.4%, 73.6% and 64.5% using 0.1% TIPA-activated SS after 28 days, and they were all below their respective regulatory limits by Standard for Pollution Control on the Hazardous Waste Landfill (GB 18598-2019) in China. Compared to the reference SS, the UCS of the treated soil at 28 days was enhanced by 237.7% using 0.1% TIPA-activated SS.

This study proposed a promising way of upcycling SS as a soil remediation agent to promote circular economy, which would not only alleviate the environmental problems of disposing SS but also provide a sustainable alternative to Portland cement in stabilization/solidification, contributing to a low-carbon future.

Declaration of Competing Interest

We declare that we do not have any commercial or associative interest that represents a conflict of interest in connection with the work submitted.

Acknowledgments

We are grateful to the financial supports by State Key Laboratory of Materials-Oriented Chemical Engineering (No.SKL-MCE-22A07), National Natural Science Foundation of China (52272018), National Key R&D Program of China (2021YFB3802002), a Project Funded by the Priority Academic Program Development (PAPD) of Jiangsu Higher Education Institutions.

References

[1] B. Zeng, Q. Wang, L. Mo, F. Jin, J. Zhu, M. Tang, Synthesis of Mg-Al LDH and its calcined form with natural materials for efficient Cr(VI) removal, Journal of Environmental Chemical Engineering, 10 (2022).

[2] M.-K. Zhang, Z.-Y. Liu, H. Wang, Use of Single Extraction Methods to Predict Bioavailability of Heavy Metals in Polluted Soils to Rice, Communications in Soil Science and Plant Analysis, 41 (2010) 820-831.

[3] Y.-L. Yang, K.R. Reddy, Y.-J. Du, R.-D. Fan, Sodium hexametaphosphate (SHMP)-amended calcium bentonite for slurry trench cutoff walls: workability and microstructure characteristics, Canadian Geotechnical Journal, 55 (2018) 528-537.

[4] Y. Yang, Reddy, KR, Du, YJ, Fan, RD, Short-Term Hydraulic Conductivity and Consolidation Properties of Soil-Bentonite Backfills Exposed to CCR-Impacted Groundwater., JOURNAL OF GEOTECHNICAL AND GEOENVIRONMENTAL ENGINEERING, 144 (2018).

[5] D. Hou, F. Li, Complexities Surrounding China's Soil Action Plan, Land Degradation & Development, 28 (2017) 2315-2320.

[6] Y. Song, N. Kirkwood, C. Maksimovic, X. Zheng, D. O'Connor, Y. Jin, D. Hou, Nature based solutions for contaminated land remediation and brownfield redevelopment in cities: A review, Sci Total Environ, 663 (2019) 568-579.

[7] C. Qu, W. Shi, J. Guo, B. Fang, S. Wang, J.P. Giesy, P.E. Holm, China's Soil Pollution Control: Choices and Challenges, Environmental science & technology, 50 (2016) 13181-13183.

[8] Z. Shen, D. Hou, B. Zhao, W. Xu, Y.S. Ok, N.S. Bolan, D.S. Alessi, Stability of heavy metals in soil washing residue with and without biochar addition under accelerated ageing, Sci Total Environ, 619-620 (2018) 185-193.

[9] Y.J. Du, M.L. Wei, K.R. Reddy, Z.P. Liu, F. Jin, Effect of acid rain pH on leaching behavior of cement stabilized lead-contaminated soil, J Hazard Mater, 271 (2014) 131-140.

[10] D. Hou, A. Al-Tabbaa, D. O'Connor, Q. Hu, Y.-G. Zhu, L. Wang, N. Kirkwood, Y.S. Ok, D.C.W. Tsang, N.S. Bolan, J. Rinklebe, Sustainable remediation and redevelopment of brownfield sites, Nature Reviews Earth & Environment, (2023).

[11] D. Hou, Q. Gu, F. Ma, S. O'Connell, Life cycle assessment comparison of thermal desorption and stabilization/solidification of mercury contaminated soil on agricultural land, Journal of Cleaner Production, 139 (2016) 949-956.
[12] J.R. Conner, S.L. Hoeffner, The History of Stabilization/Solidification Technology, Critical Reviews in Environmental Science and Technology, 28 (1998) 325-396.
[13] Z. Shen, F. Jin, D. O'Connor, D. Hou, Solidification/Stabilization for Soil Remediation: An Old Technology with New Vitality, Environ Sci Technol, 53 (2019) 11615-11617.
[14] F. Wang, F. Jin, Z. Shen, A. Al-Tabbaa, Three-year performance of in-situ mass stabilised contaminated site soils using MgO-bearing binders, J Hazard Mater, 318 (2016) 302-307.
[15] J. Shu, R. Liu, Z. Liu, H. Chen, J. Du, C. Tao, Solidification/stabilization of electrolytic manganese residue using phosphate resource and low-grade MgO/CaO, J Hazard Mater, 317 (2016) 267-274.
[16] F. Jin, Long-term effectiveness of in situ solidification/stabilization, in: Sustainable Remediation of Contaminated Soil and Groundwater, 2020, pp. 247-278.
[17] A.A.V. Cerbo, F. Ballesteros, T.C. Chen, M.-C. Lu, Solidification/stabilization of fly ash from city refuse incinerator facility and heavy metal sludge with cement additives, Environmental Science and Pollution Research, 24 (2016) 1748-1756.
[18] Z. Shen, S. Pan, D. Hou, D. O'Connor, F. Jin, L. Mo, D. Xu, Z. Zhang, D.S. Alessi, Temporal effect of MgO reactivity on the stabilization of lead contaminated soil, Environment international, 131 (2019) 104990.
[19] Y.-S. Wang, J.-G. Dai, L. Wang, D.C.W. Tsang, C.S. Poon, Influence of lead on stabilization/solidification by ordinary Portland cement and magnesium phosphate cement, Chemosphere, 190 (2018) 90-96.
[20] K.L. Scrivener, R.J. Kirkpatrick, Innovation in use and research on cementitious material, Cement and Concrete Research, 38 (2008) 128-136.
[21] Z. Shen, D. Hou, W. Xu, J. Zhang, F. Jin, B. Zhao, S. Pan, T. Peng, D.S. Alessi, Assessing long-term stability of cadmium and lead in a soil washing residue amended with MgO-based binders using quantitative accelerated ageing, Sci Total Environ, 643 (2018) 1571-1578.
[22] F. Wang, H. Wang, A. Al-Tabbaa, Leachability and heavy metal speciation of 17-year old stabilised/solidified contaminated site soils, J Hazard Mater, 278 (2014) 144-151.
[23] M.L. Wei, Y.J. Du, K.R. Reddy, H.L. Wu, Effects of freeze-thaw on characteristics of new KMP binder stabilized Zn- and Pb-contaminated soils, Environ Sci Pollut Res Int, 22 (2015) 19473-19484.
[24] Y.J. Du, N.J. Jiang, S.L. Shen, F. Jin, Experimental investigation of influence of acid rain on leaching and hydraulic characteristics of cement-based solidified/stabilized lead contaminated clay, J Hazard Mater, 225-226 (2012) 195-201.
[25] Y.-J. Du, N.-J. Jiang, S.-Y. Liu, F. Jin, D.N. Singh, A.J. Puppala, Engineering properties and microstructural characteristics of cement-stabilized zinc-contaminated kaolin, Canadian Geotechnical Journal, 51 (2014) 289-302.
[26] P. Liu, J. Zhong, M. Zhang, L. Mo, M. Deng, Effect of CO_2 treatment on the microstructure and properties of steel slag supplementary cementitous materials, Construction and Building Materials, 309 (2021).
[27] F. Han, Z. Zhang, D. Wang, P. Yan, Hydration heat evolution and kinetics of blended cement containing steel slag at different temperatures, Thermochimica Acta, 605 (2015) 43-51.
[28] B. Pang, Z. Zhou, H. Xu, Utilization of carbonated and granulated steel slag aggregate in concrete, Construction and Building Materials, 84 (2015) 454-467.

548 [29] S. Yang, J. Wang, S. Cui, H. Liu, X. Wang, Impact of four kinds of alkanolamines on hydration of
549 steel slag-blended cementitious materials, Construction and Building Materials, 131 (2017) 655-666.
550 [30] L. Mo, S. Yang, B. Huang, L. Xu, S. Feng, M. Deng, Preparation, microstructure and property of
551 carbonated artificial steel slag aggregate used in concrete, Cement and Concrete Composites, 113
552 (2020).
553 [31] S. Yang, L. Mo, M. Deng, Effects of ethylenediamine tetra-acetic acid (EDTA) on the accelerated
554 carbonation and properties of artificial steel slag aggregates, Cement and Concrete Composites, 118
555 (2021).
556 [32] J. Sun, Z. Zhang, S. Zhuang, W. He, Hydration properties and microstructure characteristics of
557 alkali–activated steel slag, Construction and Building Materials, 241 (2020).
558 [33] R. Cao, Z. Jia, Z. Zhang, Y. Zhang, N. Banthia, Leaching kinetics and reactivity evaluation of
559 ferronickel slag in alkaline conditions, Cement and Concrete Research, 137 (2020).
560 [34] Q. Wang, P. Yan, J. Yang, B. Zhang, Influence of steel slag on mechanical properties and durability
561 of concrete, Construction and Building Materials, 47 (2013) 1414-1420.
562 [35] N.K. Lee, J.G. Jang, H.K. Lee, Shrinkage characteristics of alkali-activated fly ash/slag paste and
563 mortar at early ages, Cement and Concrete Composites, 53 (2014) 239-248.
564 [36] E. Adesanya, K. Ohenoja, A. Di Maria, P. Kinnunen, M. Illikainen, Alternative alkali-activator from
565 steel-making waste for one-part alkali-activated slag, Journal of Cleaner Production, 274 (2020).
566 [37] Y. Zhou, J. Sun, Y. Liao, Influence of ground granulated blast furnace slag on the early hydration
567 and microstructure of alkali-activated converter steel slag binder, Journal of Thermal Analysis and
568 Calorimetry, 147 (2020) 243-252.
569 [38] W. Li, S. Ma, Y. Hu, X. Shen, The mechanochemical process and properties of Portland cement with
570 the addition of new alkanolamines, Powder Technology, 286 (2015) 750-756.
571 [39] Z. Xu, W. Li, J. Sun, Y. Hu, K. Xu, S. Ma, X. Shen, Research on cement hydration and hardening
572 with different alkanolamines, Construction and Building Materials, 141 (2017) 296-306.
573 [40] Z. Yan-Rong, K. Xiang-Ming, L. Zi-Chen, L. Zhen-Bao, Z. Qing, D. Bi-Qin, X. Feng, Influence of
574 triethanolamine on the hydration product of portlandite in cement paste and the mechanism, Cement
575 and Concrete Research, 87 (2016) 64-76.
576 [41] L. Chang, H. Liu, J. Wang, H. Liu, L. Song, Y. Wang, S. Cui, Effect of chelation via ethanol-
577 diisopropanolamine on hydration of pure steel slag, Construction and Building Materials, 357 (2022).
578 [42] J. Wang, L. Chang, D. Yue, Y. Zhou, H. Liu, Y. Wang, S. Yang, S. Cui, Effect of chelating
579 solubilization via different alkanolamines on the dissolution properties of steel slag, Journal of
580 Cleaner Production, 365 (2022).
581 [43] J.E.-. Research institute of highway ministry of transport, Test methods of materials stabilized with
582 inorganic binders of highway engineering, Beijing: China Communications Press, (2009).
583 [44] C. Hesse, F. Goetz-Neunhoeffer, J. Neubauer, A new approach in quantitative in-situ XRD of cement
584 pastes: Correlation of heat flow curves with early hydration reactions, Cement and Concrete Research,
585 41 (2011) 123-128.
586 [45] D. Jansen, F. Goetz-Neunhoeffer, B. Lothenbach, J. Neubauer, The early hydration of Ordinary
587 Portland Cement (OPC): An approach comparing measured heat flow with calculated heat flow from
588 QXRD, Cement and Concrete Research, 42 (2012) 134-138.
589 [46] S. Ma, W. Li, S. Zhang, Y. Hu, X. Shen, Study on the hydration and microstructure of Portland
590 cement containing diethanol-isopropanolamine, Cement and Concrete Research, 67 (2015) 122-130.
591 [47] B. Huo, B. Li, C. Chen, Y. Zhang, Surface etching and early age hydration mechanisms of steel slag

powder with formic acid, Construction and Building Materials, 280 (2021).
[48] H. Tan, Y. Guo, F. Zou, S. Jian, B. Ma, Z. Zhi, Effect of borax on rheology of calcium sulphoaluminate cement paste in the presence of polycarboxylate superplasticizer, Construction and Building Materials, 139 (2017) 277-285.
[49] Q. Wang, P. Yan, Hydration properties of basic oxygen furnace steel slag, Construction and Building Materials, 24 (2010) 1134-1140.
[50] Z. Chen, K. Tu, R. Li, J. Liu, Study on the application mechanism and mechanics of steel slag in composite cementitious materials, SN Applied Sciences, 2 (2020).
[51] D. Wang, J. Chang, W.S. Ansari, The effects of carbonation and hydration on the mineralogy and microstructure of basic oxygen furnace slag products, Journal of CO2 Utilization, 34 (2019) 87-98.
[52] China, Standard for pollution control on the hazardous waste landfill, GB 18598-2019
[53] I. Novak, Geometrical Description of Chemical Equilibrium and Le Châtelier's Principle: Two-Component Systems, Journal of Chemical Education, 95 (2017) 84-87.
[54] Q. Wang, M. Li, J. Yang, J. Cui, W. Zhou, X. Guo, Study on mechanical and permeability characteristics of nickel-copper-contaminated soil solidified by CFG, Environ Sci Pollut Res Int, 27 (2020) 18577-18591.
[55] W. Li, P. Ni, Y. Yi, Comparison of reactive magnesia, quick lime, and ordinary Portland cement for stabilization/solidification of heavy metal-contaminated soils, Sci Total Environ, 671 (2019) 741-753.
[56] L. Sha, Z. Zou, J. Qu, X. Li, Y. Huang, C. Wu, Z. Xu, As(III) removal from aqueous solution by katoite (Ca(3)Al(2)(OH)(12)), Chemosphere, 260 (2020) 127555.

Alkanolamines-activated steel slag for stabilization/solidification of heavy metal contaminated soil

Bin Zeng[b], Zhi Zhang[b], Shuo Yang[b], Liwu Mo[a,b,*], Fei Jin[c]

[a] *State Key Laboratory of Materials-Oriented Chemical Engineering, Nanjing Tech University, Nanjing, Jiangsu 211800, PR China*

[b] *College of Materials Science and Engineering, Nanjing Tech University, Nanjing, Jiangsu 211800, PR China*

[c] *School of Engineering, Cardiff University, CF24 3AA, UK*

E-mail address: andymoliwu@njtech.edu.cn

Highlights:

- Alkanolamines promoted the hydration of steel slag and with TIPA showing the best performance.
- The UCS of treated HM-contaminated soil at 28 days was more than tripled using 0.1% TIPA-activated SS compared to the non-activated SS.
- TCLP leached concentrations of Cd, Cu, Ni, Pb, and Zn were reduced by 87.2%, 78.8%, 62.4%, 73.6% and 64.5% using 0.1% TIPA-activated SS at 28 days.
- Alkanolamines-activated SS is a sustainable alternative to PC in S/S for heavily-contaminated soil

Abbreviations:

SS: Steel slag **S/S**: Stabilization/Solidification **HM**: Heavy metals
TEA: Triethanolamine **TIPA**: Triisopropanolamine **EDIPA**: Ethyldiisopropylamine
DEIPA: Diethanolisopropanolamine **UCS**: Unconfined compressive strength
β-C_2S: β-larnite **$CaCO_3$**: Calcite **C_2F**: Srebrodolskite **$C_{12}A_7$**: Mayenite
C_3A: Tricalcium aluminate **C-S-H**: Calcium silicate hydrate **Mc**: Monocarboaluminate
CH: Portlandite **C-A-H**: Calcium aluminate hydrate **C-F-H**: Calcium ferrite hydrate
IC: Isothermal calorimetry **XRD**: X-ray diffraction **TGA**: Thermogravimetric analysis
TCLP: Toxicity Characteristic Leaching Procedure

~~**Abstract:** Steel slag (SS) is a byproduct discharged from steel-making industry and has not been well utilized in contaminated soil stabilization/solidification (S/S) due to its low hydration activity. In this study, four different alkanolamines (TEA, TIPA, EDIPA and DEIPA) were used to activate SS and improve its cementitious properties and metal binding performance. The activated SS was used to treat contaminated soils containing HM (heavy metals) of Cd, Cu, Ni, Pb and Zn. Compared~~

~~with the reference SS without activators, alkanolamines-activated SS showed better S/S performance in terms of strength and leaching, and the performance was improved by increasing the activator dosage. For instance, concentrations of leached Cd, Cu, Ni, Pb, and Zn have reduced by 87.2%, 78.8%, 62.4%, 73.6% and 64.5% by using 0.1% TIPA-activated SS after 28 days, and they were all below their respective regulatory limits by Standard for Pollution Control on the Hazardous Waste Landfill (GB 18598-2019) in China. Compared to the reference SS, the unconfined compressive strength (UCS) of the treated soil at 28 days was enhanced by 237.7% using 0.1% TIPA-activated SS. To elucidate the activation mechanism, the hydration process of SS was thoroughly followed via isothermal calorimetry (IC) and conductivity analysis, and the nature of hydration products was studied by X-ray diffraction (XRD) and thermogravimetric analysis (TGA). It was concluded that alkanolamines facilitated the dissolution of minerals in SS and formation of hydration products (e.g., C-S-H, C-A-H, C-F-H and Mc), and hence significantly enhanced the microstructural development and engineering properties of SS. This work demonstrated a promising way of upcycling SS as an effective S/S agent for handling complex heavy metal contaminated soil.~~

Abstract: Steel slag (SS) is a byproduct discharged from steel-making industry with less than 25% utilization rate in China. The low utilisation rate of SS is associated with its low hydration activity in cement and concrete. In this study, four different alkanolamines (TEA, TIPA, EDIPA and DEIPA) were used to activate SS to improve its cementitious properties and metal binding performance, and hence its capacity on treating heavy metal-contaminated soils containing Cd, Cu, Ni, Pb and Zn. Compared with the reference SS without activators, concentrations of leached Cd, Cu, Ni, Pb, and Zn have reduced by 87.2%, 78.8%, 62.4%, 73.6% and 64.5% by using 0.1% TIPA-activated SS after 28 days, and they were all below their respective regulatory limits by Standard for Pollution Control on the Hazardous Waste Landfill (GB 18598-2019) in China, and the unconfined compressive strength (UCS) of the treated soil at 28 days was enhanced by 237.7% using 0.1% TIPA-activated SS. To elucidate the activation mechanism, the hydration process of SS was thoroughly followed via isothermal calorimetry (IC) and conductivity analysis, and the nature of hydration products was studied by X-ray diffraction (XRD) and thermogravimetric analysis (TGA). It was concluded that alkanolamines facilitated the dissolution of minerals in SS and formation of

hydration products (e.g., C-S-H, C-A-H, C-F-H and Mc), and hence significantly enhanced the microstructural development and engineering properties of SS. This work demonstrated a promising way of upcycling SS as an effective and sustainable S/S agent for handling complex heavy metal contaminated soil, with the potential of enhancing the SS utilization significantly.

Keywords: Alkanolamines, Steel slag activation, Heavy Metals, Soil Stabilization/Solidification

1. Introduction

Globally, heavy metals (HM) discharged from metal casting industries, fossil fuel burning, and the ever-growing use of gasoline, paint, chemical fertilizer and pesticide have been accumulating in soils in the past few decades[1]. Heavy metal-contaminated soil has become one of the most serious environmental issues all over the world, threatening human health [2-4]. A national soil survey found that in China 16.1% of the surveyed land exceeded national standards of soil contamination, within which 19.4% of agricultural land and 34.9% of former industrial land were regarded as contaminated [5-7], with HM as the most prevalent contaminants. HM such as cadmium (Cd), copper (Cu), nickel (Ni), lead (Pb), and zinc (Zn) are highly toxic [8, 9]. Effective and sustainable soil remediation technologies have been developed to treat HM-contaminated soil and achieved great successes in the past few years[10].

Stabilization/solidification (S/S) is the most widely-used technology in China to treat HM-contaminated soil (48.5% adoption rate in the 2017-2018 year) [11-13]. The method involves using binders to immobilize heavy metals in contaminated soil through physical encapsulation, adsorption and chemical reactions, which decrease the bioavailability/ecotoxicity of the contaminants and improve the engineering properties of the contaminated soils [14-16]. Previous studies had highlighted the effectiveness of using highly alkaline cementitious materials in S/S, such as Portland cement (PC), MgO-based materials and lime-fly ash blends [17-19]. However, the production of these traditional binders was associated with intensive consumption of energy and nonrenewable resources, and contributed to ~10% of anthropogenic greenhouse gas emissions [20]. Furthermore, the high-alkaline binders may have adverse effects including incompatibility with HM, elevated soil pH and high HM leachability, particularly under aggressive environmental conditions [21-24], which limited the effectiveness of them in treating heavily-contaminated soils [25]. Therefore, it is always desirable to develop alternative binders with higher efficiency, better stability, low-cost and more environmentally friendly to remediate contaminated soils [12].

Steel slag (SS) is an alkaline industrial waste produced during the steelmaking process with an annual production of approximately 15-20 wt% of the total steel output worldwide [26, 27]. In China, the annual output of SS exceeded 100 million tons which accounted for approximately 24% of Chinese total industrial solid waste; nonetheless, its utilization rate is less than 25% [28]. Therefore, the large-scale utilization of SS is urgently needed as its disposal caused serious environmental pollution and occupied valuable lands [29]. Depending on the steelmaking method, the main chemical composition of SS is SiO_2, CaO, Al_2O_3, Fe_2O_3 and MgO. In terms of mineral forms, SS mainly consists of tricalcium silicate (C_3S), dicalcium silicate (C_2S), C_4AF, $C_{12}A_7$, C_2F, RO phase (metal oxides solid solution), free CaO and free MgO [30-33]. The composition of SS is similar to PC which shows its potential to be utilized as an alternative green binder in S/S for treating HM-contaminated soil. However, the hydration activity of SS is much lower than that of PC [34], which necessitates its activation prior to its application in S/S.

Alkali activation has been widely used to improve the hydraulic properties of SS using water glass, sodium hydroxide, sodium silicate and sodium sulfate, etc. [35, 36]. However, the production of those strong alkalis is not only associated with huge CO_2 emissions but also costly for large-scale SS utilization [37]. Additionally, owing to the ultra-high alkalinity of the alkali activators, the alkali-activated SS would also elevate the soil alkalinity and hence adversely impact the ecological balance of the environment. Therefore, developing a low-cost, environment friendly and effective activator for SS would pave the way for its application in HM-contaminated soil remediation.

Recently, it has been reported that alkanolamines could affect the structure of hydration products in PC, and different types of alkanolamines exhibited different impacts [38-40]. Other researchers also found that alkanolamines could promote the hydration and chelating solubilization of SS [41, 42]. Thus, alkanolamines activated SS may serve as a promising alternative binder to remediate HM-contaminated soil considering: (i) the potential large-scale utilisation of SS which would reduce the negative environmental impact of SS accumulation; (ii) enhancement of the hydration of SS for improved S/S performance, particularly the early-age properties; (iii) the low cost and low carbon footprint of SS compared to PC. However, none has examined the performance of alkanolamines-activated SS for HM-contaminated soil remediation yet and there is a lack of understanding on the activation mechanism and optimal dosage of this new type of activator (i.e. alkanolamines) for SS.

In this study, detailed analyses were conducted on the hydration kinetics, hydration products and strength of the hydrated SS by different alkanolamines including triethanolamine (TEA), triisopropanolamine (TIPA), ethyldiisopropylamine (EDIPA) and diethanolisopropanolamine (DEIPA) using characterization methods such as X-ray diffraction (XRD), isothermal calorimetry, thermogravimetric analysis (TGA) and Fourier transform infrared spectroscopy (FT-IR). The performance (i.e., strength and leachability of HM) of activated-SS treated HM-contaminated soils was assessed within 180 days to investigate the temporal effect of the type and dosage of the activators.

2. Materials and methods

2.1 Preparation of binders

The SS used in this study was derived from the Meishan Iron & Steel plant in China. Raw SS lumps were crushed, ball milled and then passed through a 20-mesh screen to obtain the SS powder, with its chemical compositions presented in Table 1. Both the concentrations of Cr and V ions in the TCLP leachates were below the detection limits indicating the low leachability of the two potential contaminants from the SS. The mineral components of the SS were examined by XRD (Fig. 1), which shows that the it mainly consists of β-larnite (β-C_2S), Calcite ($CaCO_3$), srebrodolskite (C_2F), mayenite ($C_{12}A_7$), tricalcium aluminate (C_3A).

Fig. 2 shows the chemical structures of the four types of alkanolamines (AR grade) used in this work, of which the TEA and TIPA were provided by Aladdin corporation, and EDIPA and DEIPA were provided by Hongbaoli Co., Ltd. The activators were combined with SS powders according to the proportions in Table 2 and then milled in a planetary ball mill at a speed of 220 r/min for 30 min to obtain the activated SS.

Table 1

Chemical compositions of SS measured by XRF.

Chemical composition (wt%)	CaO	Fe_2O_3	SiO_2	Al_2O_3	MgO	MnO	P_2O_5	TiO_2	Cr_2O_3	V_2O_5	LOI
Steel slag	35.89	25.49	14.77	8.23	6.30	3.55	2.32	0.97	0.24	0.21	1.12

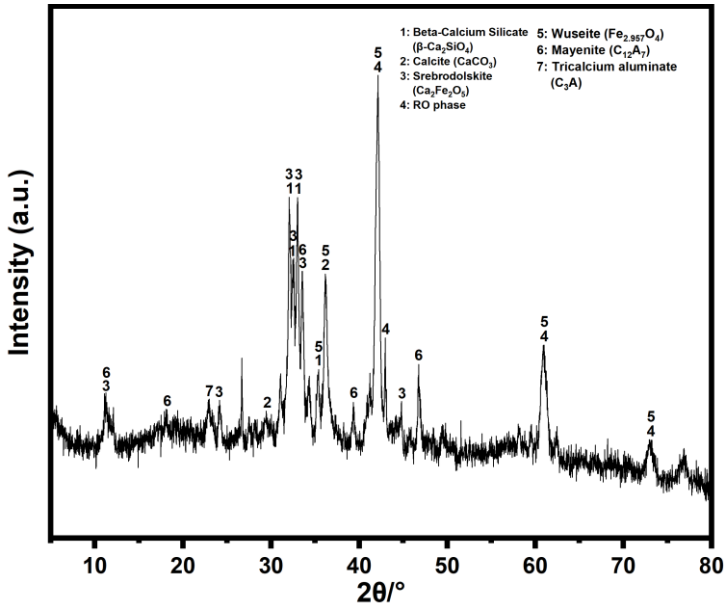

147

148 **Fig. 1** XRD pattern of SS

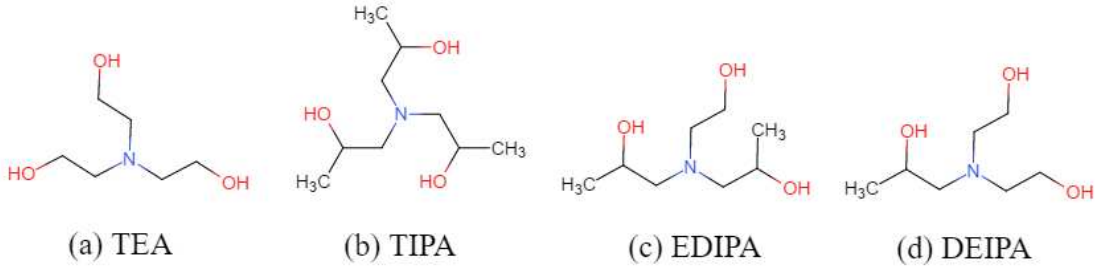

149

150 **Fig. 2** Schematic representation of the molecular structures of the four alkanolamines used in this study

151 **Table 2**

152 The type and content (by weight of SS) of alkanolamines used as activators

	Alkanolamines	Content (%)
Control	None	-
TIPA-0.02	TIPA	0.02
TIPA-0.05	TIPA	0.05
TIPA-0.08	TIPA	0.08
TIPA-0.1	TIPA	0.1
TEA-0.05	TEA	0.05
EDIPA-0.05	EDIPA	0.05
DEIPA-0.05	DEIPA	0.05

153 *2.2 Mechanistic study on the activation of SS by alkanolamines*

154 *2.2.1 Compressive strength tests of activated SS paste*

155 The SS pastes activated by alkanolamines with water to solid ratio of 0.2 were prepared and cast in

156 20 mm × 20 mm × 20 mm moulds. These samples were cured in a moist cabinet under the condition

157 of 20 ± 1 ℃, 95 ± 1% relative humidity for 24h, and then demoulded and placed in the isothermal

158 curing cabinet under the same condition until the testing age (1d, 3d, 7d, 28d, 90d and 180d). The
159 mean compressive strength of six cement pastes was recorded for each mix. The crushed samples
160 were ground, sieved and then immersed in ethanol for terminating hydration, followed by drying at
161 60°C for 24 h in a vacuum oven until further characterization.
162 *2.2.2 Isothermal calorimetry*
163 The hydration heat of activated SS was measured by a Thermometric TAM Air isothermal
164 calorimeter (TA Instruments) at 20 ± 0.02 ℃. Approximately 4 g of dry powders were loaded in
165 glass ampoules, and syringes were loaded with 2 g of water. When a steady baseline was reached,
166 the solution was injected into glass ampoules and externally stirred for 20 s. Then the glass ampoule
167 was sealed and placed into the isothermal calorimeter. The heat of hydration was measured for 3
168 days to study the effect of activator on the hydration of SS.
169 *2.2.3 Liquid phase conductivity*
170 The dissolution rates of the reference and activated SS were followed by measuring the
171 conductivities of the SS slurries. The slurries were prepared by mixing the SS and water with a
172 liquid/solid ratio of 5. The magnetic stirrer was used for the mixing process at 250 rpm and stirred
173 for 48h. The conductivities of the slurries were continuously recorded by a conductivity meter
174 (DDSJ-308A, made in Shanghai Yueping).
175 *2.2.4 X-ray diffraction (XRD)*
176 XRD analysis was conducted on D/max-2500 X-ray diffraction of Rigaku, Japan, with CuKα
177 radiation, 40 kV voltage, 200 mA current, 2θ between 5°and 80°, 0.02°/s scan speed and 0.02° step
178 size to characterize the mineralogical phases of SS at different ages.
179 *2.2.5 Thermogravimetry/differential scanning calorimetry (TG-DTG)*
180 Thermogravimetric and differential thermogravimetric analysis (TG/DTG) was operated under N_2
181 flow with heating rate of 10℃/min from the ambient temperature to 1000℃ using STA409C
182 instrument of NETZSCH.
183 *2.3 Preparation of contaminated soils*
184 A clean soil was obtained by sampling a surface soil up to 50 cm depth from Xinxiang of Henan
185 Province, China, and dried in an oven at 105℃ for 6 hours. The dried soil was crushed, ground and
186 then passed through a 1 mm sieve and stored in a polyethylene container for the subsequent

physicochemical properties tests and the results were shown in Table 3. HMs were not leached from clean soil and SS used in the experiments by the TCLP method. In this work, a heavily HM-contaminated soil was prepared via doping Cd, Cu, Ni, Pb and Zn (in the form of $Cd(NO_3)_2{\cdot}4H_2O$, $Cu(NO_3)_2 \cdot 3H_2O$, $Ni(NO_3)_2 \cdot 6H_2O$, $Pb(NO_3)_2$, $Zn(NO_3)_2 \cdot 6H_2O$ respectively, AR grade from Sinopharm Chemical Reagent Co., Ltd.) to the clean soil. Predetermined amounts of HM (i.e., 24 mg/kg of Cd, 10000 mg/kg of Cu, 500 mg/kg of Ni, 280 mg/kg of Pb and 12500 mg/kg of Zn by weight of dry soils) were firstly dissolved into the solution and added to the dry soil (to keep the moisture content at 20%) and then stirred vigorously for 30 min to prepare the co-contaminated soil. The mixture was sealed and kept for 24 hours to ensure the adequate distribution of HM in soil. The binder and water were then added and mixed to achieve homogeneity. The weight ratio of binder to soil is 2:8 and the final weight ratio of water to solid (including soil and binder) was determined as 25:100 since preliminary results showed that consistencies of the mixtures were optimal at this level (i.e., neither too dry nor too wet for handling). After that, approximately 200 g of the mixture was statically compacted by a stainless steel cylindrical mold with 50 mm diameter and 50 mm height. Then, the specimen was carefully extruded from the mold using a hydraulic jack and sealed in a polyethylene bag for curing under the standard condition (temperature 20 ± 2 ℃, relative humidity 99%). Specimens were collected for various tests at ages of 1, 3, 7, 28, 90 and 180 days.

Table 3

Basic physicochemical properties of the soil

Property	Value[b]	Test method
Specific gravity, G_s	2.59	ASTM D854-14
Liquid limit, w_L (%)	33.4	ASTM D4318-10
Plastic limit, w_P (%)	17.2	ASTM D4318-10
Optimum water content, w_{opt} (%)	21.8	ASTM D698-12
Maximum dry density, ρ_d (g/cm^3)	1.82	ASTM D698-12
Average soil pH	8.19	ASTM D4972-13
Soil classification	CL	ASTM D2487-11
Grain size distribution (%)[a]		-
Clay (<0.002 mm)	22.5	
Silt (0.002–0.075 mm)	51.7	
Sand (0.075–2 mm)	25.8	

[a] Measured using a laser particle size analyzer Mastersizer 2000 (Malvern, USA).

[b] Number of replicate = 3, and coefficient of variance (COV) < 5%.

2.4 Unconfined compressive strength (UCS) tests for contaminated soils

The microcomputer-controlled electronic universal testing machine of Shanghai Yihuan Instrument Technology Co., Ltd was used to assess the UCS of contaminated soils according to JTG E51-2009[43], at a speed of 1 mm·min^{-1}. The mean UCS of six soil samples was recorded for each mix and presented here. The crushed samples were collected, ground and sieved through a 4 mm mesh before leaching tests.

2.5 Leaching test for contaminated soils

After incubation for designated time periods, specimens were firstly dried at 65 ℃ to achieve constant weights. The leachabilities of Cd, Cu, Ni, Pb and Zn in the samples was evaluated according to US EPA Method 1311 - Toxicity Characteristic Leaching Procedure (TCLP). Briefly, approximately 5 g of the crushed sample was added to ~96.5 mL deionized water and stirred for 5 min and the pH value (which determines buffer solution chose) of the mixture was recoded with a pH meter (Rex PHS-3E). The soil and buffer solution (HOAc/NaOAc, pH 4.93) were mixed with a solid/liquid ratio of 1:20 in a 2 L polyethylene bottle and shaken at 250 rpm for 18 h. Cd, Cu, Ni, Pb and Zn concentrations in the filtrates were measured by ICP-OES after filtration with 0.45μm filter, dilution (if necessary) and acidification to pH < 2.

2.6 Statistical analysis

All compressive strength experiments were carried out in sextuplicate, and leaching experiments were carried out in triplicate. The mean and standard deviations of each experiment were presented. The significance of differences between groups was determined by one-way ANOVA using Duncan method with a significance level of 0.05 using SPSS 17, and indicated by different lowercase letters in the figures.

3. Results

3.1 Hydration properties of alkanolamine-activated SS

As the capacity to solidify and stabilize HM was closely related to the binder's hydration characteristics, the following sections will focus on the hydration mechanisms and evolution of mineral compositions of the alkanolamine-activated SS.

3.1.1 Heat evolution

The reaction of SS with water was a thermodynamic reaction accompanied by exothermic behavior,

237 which could be recorded using conduction calorimetry. The heat release curves were characterized
238 by the presence of two peaks. The initial peak was attributed to the dissolution of f-CaO, C_3A and
239 $C_{12}A_7$ [44, 45], leading to the continuous accumulation of ions. When the ion concentrations reached
240 a certain level, the second exothermic peak appeared, ascribed to the precipitation of the CH
241 (portlandite) and C-S-H (calcium silicate hydrate) phases [46] and the dissolution of β-C_2S and C_2F
242 [47]. The hydration process gradually stabilized after the second exothermic peak.
243 Fig. 3 shows the effect of different alkanolamines on the hydration heat evolution rate and
244 cumulative hydration heat of SS. All the alkanolamines increased the heat generation significantly.
245 No significant difference was observed for the appearance time of the first exothermic peak, while
246 the second peak appeared the earliest for TEA and latest for TIPA. The second peak was not
247 observed for the control sample, which is likely due to the low hydration reactivity of the SS used
248 in this work and hence the 2nd peak may appear beyond 72 hours.
249 Fig. 4 presents the effect of TIPA dosage on the hydration heat evolution rate and cumulative
250 hydration heat. The first peak increased significantly with the increased TIPA content indicated that
251 a higher dosage of TIPA improved the dissolution of mineral phases. Moreover, higher TIPA dosage
252 shortened the induction period for the second peak, implying that time had reduced for the ion
253 concentrations to reach supersaturation with the addition of more TIPA. The cumulative hydration
254 heat increased proportionally with the dosage of TIPA.

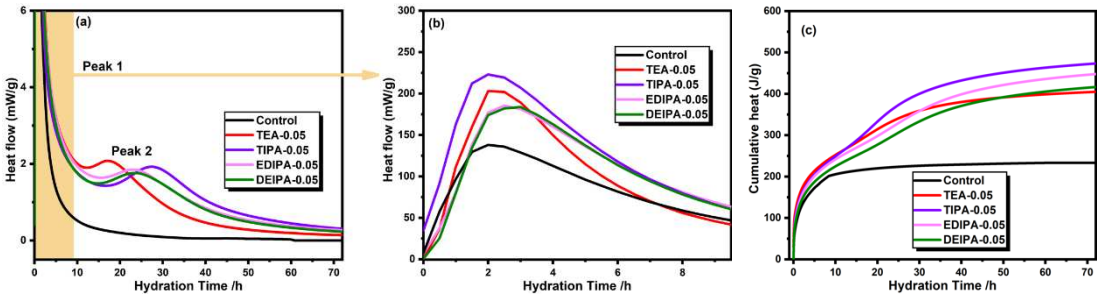

255
256 **Fig. 3** Hydration heat evolution of different alkanolamines-activated SS: (a) Heat flow of the whole hydration
257 process, (b) heat flow in the first 9 h (Peak 1) and (c) cumulative hydration heat.

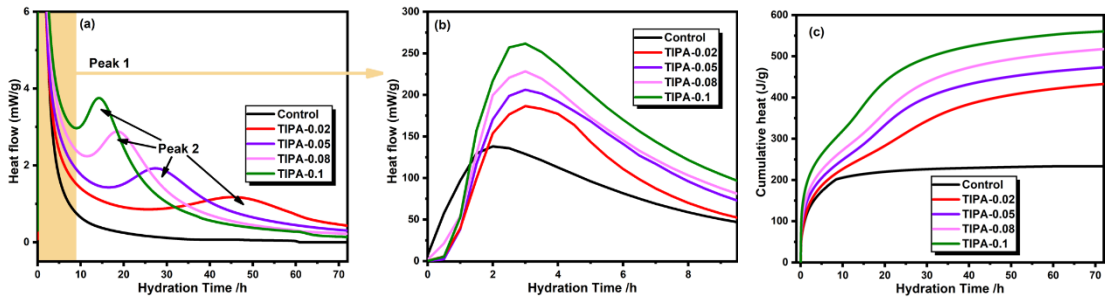

Fig. 4 Hydration heat evolution of TIPA-activated SS at different TIPA dosages: (a) Heat flow of the whole hydration process, (b) heat flow in the first 9 h (Peak 1) and (c) cumulative hydration heat.

3.1.2 Conductivity of SS slurries

The ion concentrations in the aqueous phase could be indirectly assessed by measuring the conductivity of the solution, which could be used to evaluate the dissolution rate of SS [48]. Fig. 5 shows the evolution of conductivity in the SS slurries with and without alkanolamines. The conductivity reached the peak at the first 5 min due to the dissolution of the high solubility mineral phases (e.g., free lime and aluminates). This was followed by the ionic reactions in the solution leading to rapidly decreased conductivity. After approximately 60 min, the conductivities of the SS solutions with activators rose again and then dropped gradually over time, while this second peak was not observed in the control sample. Apparently, the activators promoted the dissolution of SS again when the ion concentration dropped, which induced the second peak.

For the control sample, the precipitation of the hydration products continuously consumed the dissolved ions. Meanwhile, the dissolved cations adsorbed on the surface of SS particles and formed a coating layer, which was not conducive to further dissolution [49]. This explains the gradually decreased conductivity and higher residual conductivity over time due to the diffusion-controlled dissolution of SS particles over time, ascribed to the surface coating. With the addition of alkanolamines, the chelating of cations led to exposed SS surface for further dissolution, which was evidenced by the second peak. Moreover, chelation likely resulted in higher supersaturation degrees of the ions in the solution, which induced more hydration/precipitation products. This is the reason of the much lower residual conductivities of the SS samples with activators. Among the four alkanolamines, TIPA showed the highest second peak and lowest residual conductivity, indicating its best performance as the chelating agent for promoting the hydration of SS. Fig. 5 (b) shows that the effect of TIPA is highly correlated with its dosage. Increasing the dosage from 0.02% to 0.1%

proportionally increased the conductivity of the second peak and reduced the residual conductivity of the solution.

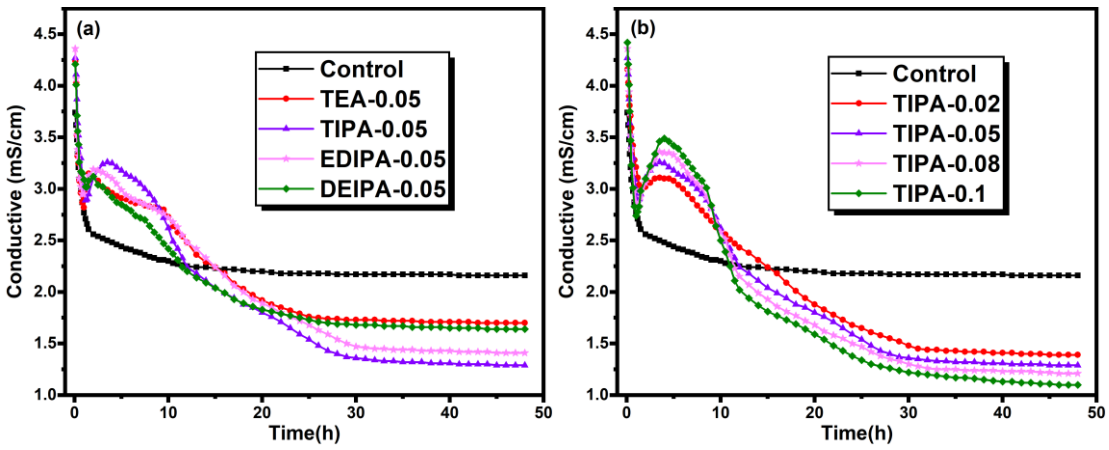

Fig. 5 Evolution of conductivity in the SS solutions with and without alkanolamines: (a) SS with four different alkanolamines at the same dosage of 0.05%, (b) SS with 0.02%, 0.05%, 0.08% and 0.1% TIPA.

3.1.3 XRD

The hydration products were characterized by XRD in Fig. 6. Compared with unhydrated SS (Fig. 1), the peaks of C_3A disappeared and the peaks of β-C_2S, C_2F, $C_{12}A_7$ and $CaCO_3$ weakened. Moreover, the peaks of hydration products such as $Ca_3Fe_2Si_{1.15}O_{4.6}(OH)_{7.4}$, $Ca_3Al_2(O_4H_4)_3$ and $C_4(A,F)\check{C}H_{11}$ appeared, which could be formed by the hydration of C_3A, $C_{12}A_7$, C_2F and $CaCO_3$. Moreover, hydration of β-C_2S would form C-S-H and these hydration products would potentially contribute to the cementitious and metal-binding capability in soil S/S. As shown in Fig. 6 (a), the peaks of hydration products of activated SS were stronger than those of SS without activators. The enlarge view ($2\boldsymbol{\theta}$ = 31.5°-34.0°) clearly exhibits that the characteristic peaks of β-C_2S and C_2F weakened further after the addition of activators, indicating higher dissolution/reaction rates of these mineral phases. Consistent with the conductivity results, SS activated by TIPA exhibited the lowest peaks of β-C_2S, C_2F and highest peaks of the hydration products compared with other activators. Fig. 6 (b) further demonstrated that the dissolution of the minerals in SS and the precipitation of the hydration products were promoted by the increased dosage of TIPA from 0.02% to 0.1%.

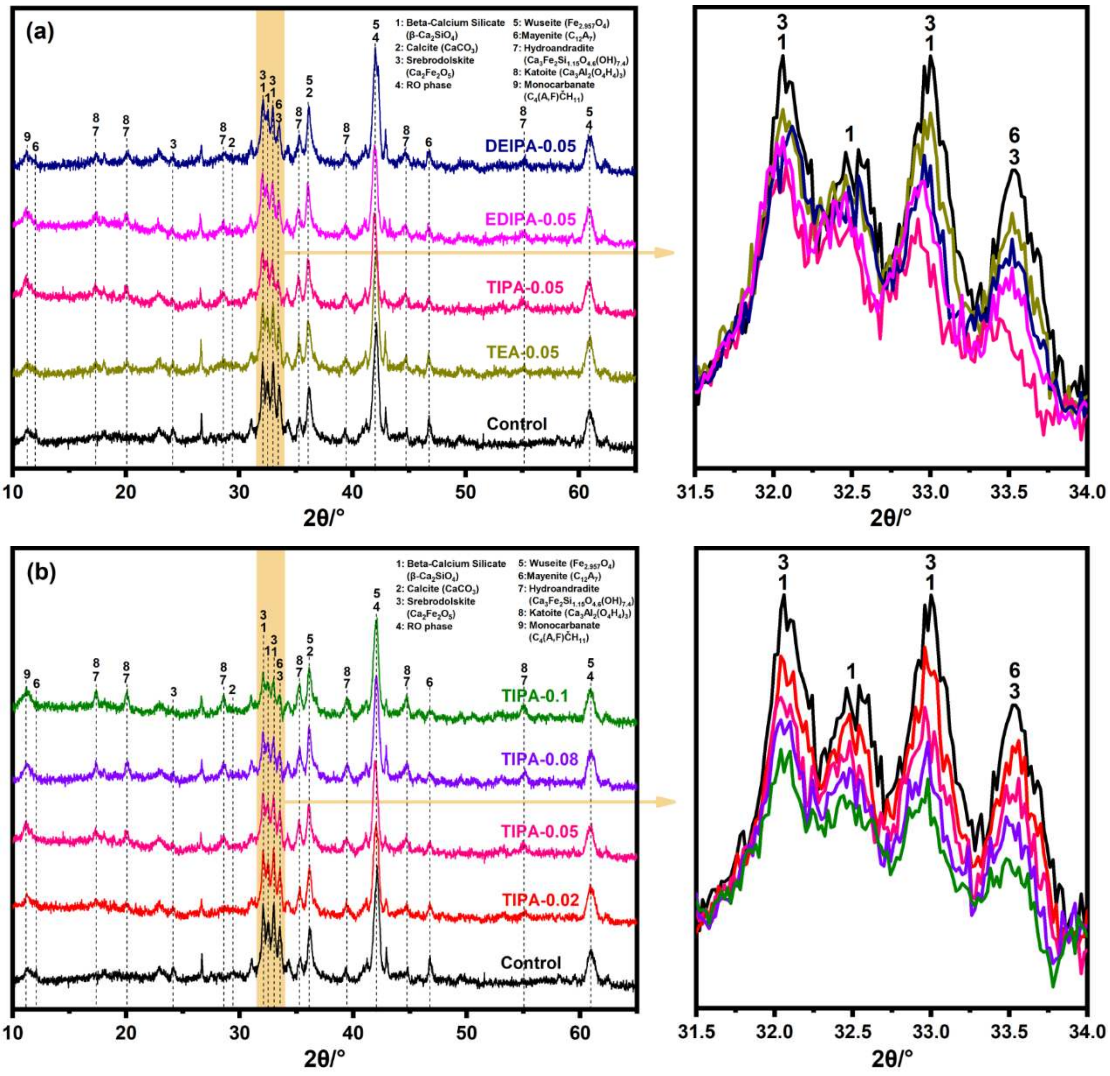

Fig. 6 XRD patterns of phase compositions in hardened SS pastes at 28 days activated by: (a) four different alkanolamines, (b) 0.02%, 0.05%, 0.08% and 0.1% TIPA.

3.1.4 Thermogravimetric analysis (TGA)

During SS hydration, mineral phases reacted with water to form hydration products, and hydration products were readily carbonated to form corresponding carbonates. In order to investigate the effects of activator type and dosage on the hydration of SS, the hydration products of SS paste were characterized by TGA as shown in Fig. 7. It could be seen from the derivative thermogravimetric (DTG) curve that there were mainly three mass loss peaks. The peak at ~140 ℃is mainly due to the dehydration of C-S-H gel and Mc (monocarboaluminate). The peak at ~280 ℃is mainly ascribed to the dehydration of C-A-H (calcium aluminate hydrate) and C-F-H (calcium ferrite hydrate) [29, 50]. In the range of 650-750 ℃, the peak is mainly due to the decarbonation of $CaCO_3$ [51]. C-S-H gel was generated from the hydration of silicate phases, C-A-H and Mc from aluminates, and C-F-H

from C_2F. Moreover, a portion of $CaCO_3$ was reacted and produced Mc.

Fig. 7(a) showed the TG and DTG curves of the SS pastes at the age of 28 days activated by the four alkanolamines. Compared with the control sample, the first two peaks were much more pronounced in the samples with activators, while the one associated with $CaCO_3$ was weaker. Moreover, TIPA-activated SS showed the maximum weight losses due to C-S-H, Mc, C-A-H and C-F-H decomposition and the minimum weight loss of $CaCO_3$ decomposition. In Fig. 7(b), higher dosage of TIPA increased the peaks associated with hydration products while decreased the one with $CaCO_3$. The TGA results agreed well with other tests on the best activation performance of TIPA and the enhanced effect by increasing its dosage.

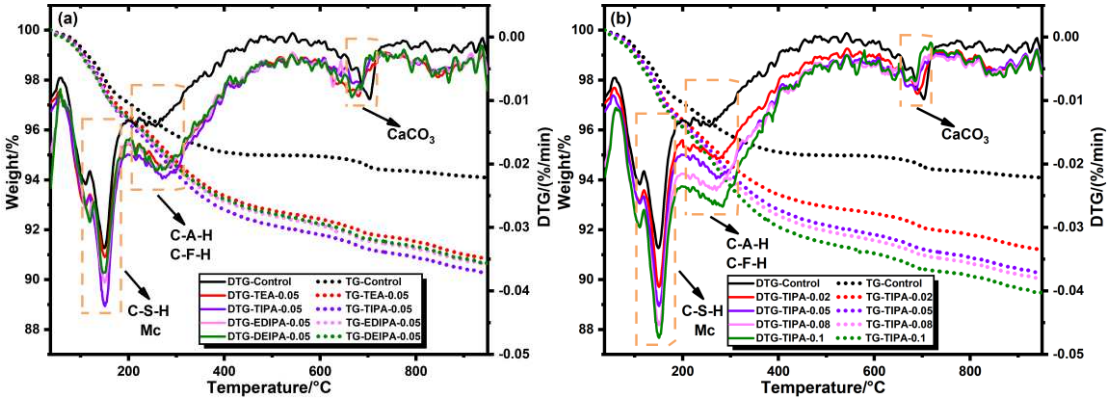

Fig. 7 TG-DTG curves of hardened SS pastes at 28d activated by: (a) four different alkanolamines at the same addition dosage of 0.05%, (b) 0.02%, 0.05%, 0.08% and 0.1% TIPA.

3.2 Compressive strength of alkanolamine-activated SS pastes

The effects of four different alkanolamines on the mechanical properties of hardened SS pastes were evaluated by measuring the compressive strength of SS pastes at different ages as shown in Fig. 8(a). It could be seen that the compressive strength gradually increased with curing time with the rate decreased. Moreover, the activators significantly improved the compressive strength of the hardened SS pastes with the effectiveness decreasing in the order of TIPA>EDIPA>DEIPA>TEA. Specifically, at 28d, the compressive strength of the SS paste without activators was only 14.8 MPa, which was increased to 27.1, 34.6, 30.9 and 28.6 MPa after adding 0.05 % TEA, TIPA, EDIPA and DEIPA, respectively. Fig. 8(b) showed the effect of TIPA dosage on the compressive strength, demonstrating the positive correlation between TIPA dosage and the improvement of compressive strength, agreeing well with the increased quantities of hydration products. It is worth noting that adding only 0.1% of TIPA to SS enhanced the compressive strength by ~190% and ~140% at 28d

and 180d, respectively.

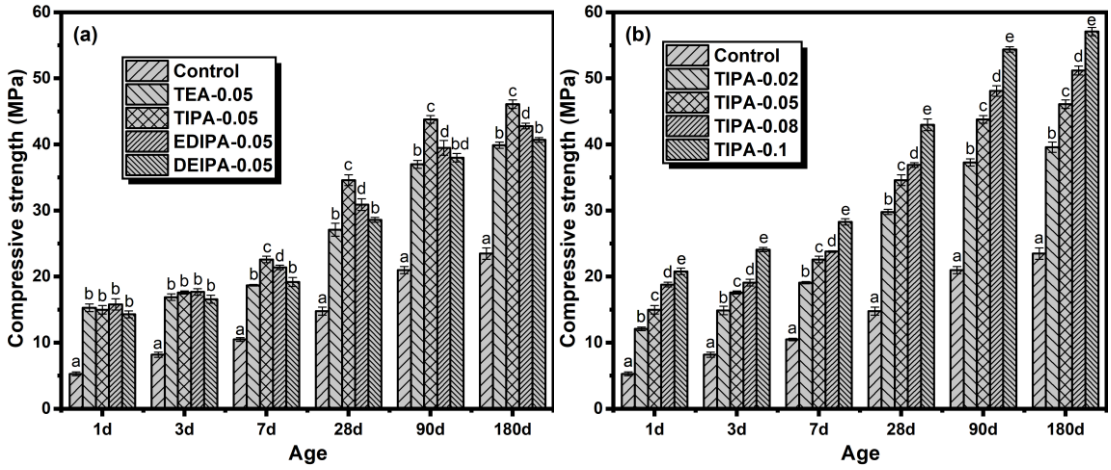

Fig. 8 Effect of activators on compressive strength of activated SS pastes: (a) four alkanolamines (TEA, TIPA, EDIPA and DEIPA) at the same dosage of 0.05% and (b) 0.02%, 0.05%, 0.08% and 0.1% TIPA.

3.3 UCS of activated-SS treated HM-contaminated soil

The UCS test has been widely used to describe the mechanical properties of S/S soils. The type of binder and curing age have significant impacts on the physicochemical properties of the HM-contaminated soil treated with S/S. In general, the development of UCS of treated soils was consistent with the results of the paste samples (comparing Fig.9 and Fig. 8). All the activators showed excellent performance in the presence of high concentrations of multiple HMs in the soils. TIPA-activated SS exhibited the highest strength among all the alkanolamines (Fig. 9a) and its effect on UCS was positively correlated with the dosage (Fig. 9b). The UCS results demonstrated that by adding as low as 0.02% of TIPA to SS, the strength could be improved by more than 100% at all ages, which showed their excellent compatibility with HMs and great promise to reduce the use of SS usage in contaminated soil S/S.

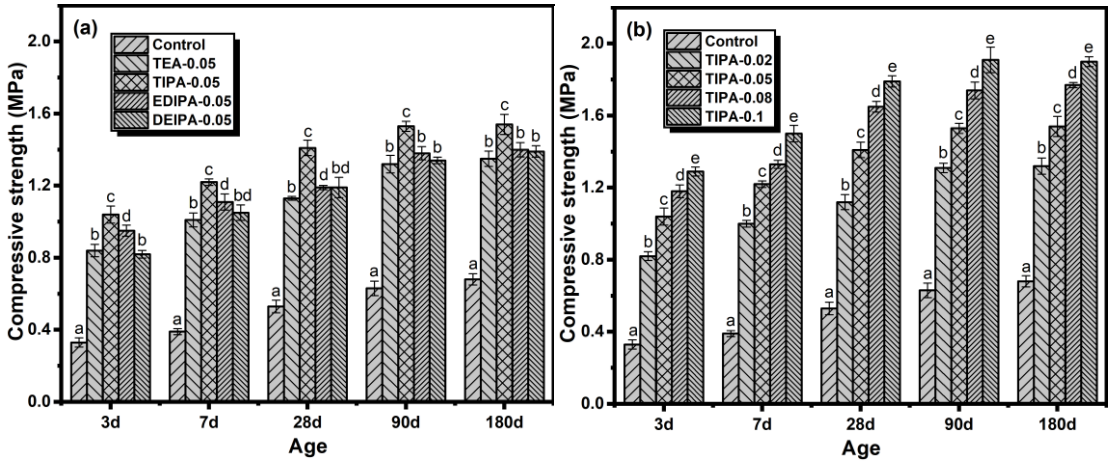

Fig. 9 Effect of activated-SS on the UCS of HM-contaminated soil: (a) four alkanolamines (TEA, TIPA, EDIPA and DEIPA) at the same dosage of 0.05% and (b) 0.02%, 0.05%, 0.08% and 0.1% TIPA.

3.4 TCLP results of activated-SS treated HM-contaminated soil

3.4.1 Effect of different alkanolamines

The concentrations of leached HM, i.e., Cd, Cu, Ni, Pb and Zn in contaminated soils treated by alkanolamine-activated SS were shown in Fig. 10. Apparently, the leachability of all the HM were significantly reduced after S/S over time, which indicated that SS exhibited superior capacity in solidifying and stabilizing the HM in the contaminated soil. With activators, the effectiveness of HM stabilization was improved, while the type of activator did not seem to influence the early-age leachability of HM significantly up to 7 days. Above 28 days, TIPA and EDIPA showed the best performance among all the alkanolamines for the TCLP results. Moreover, it is worth noting that 0.5% of TIPA successfully lowered the leached concentrations of all the HM (except for Ni, which barely exceeded the limit) to below their regulatory limits (see Standard for Pollution Control on the Hazardous Waste Landfill (GB 18598-2019) [52]) in China after curing of 28 days.

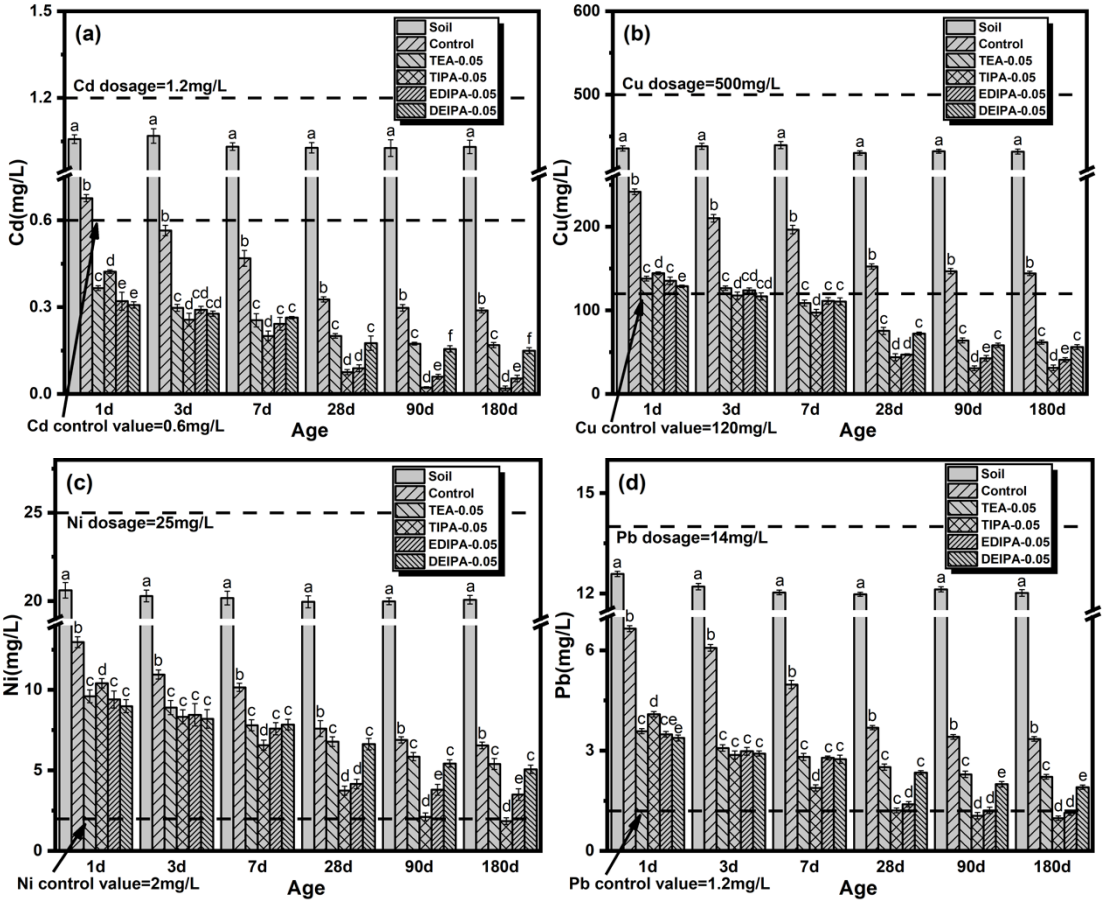

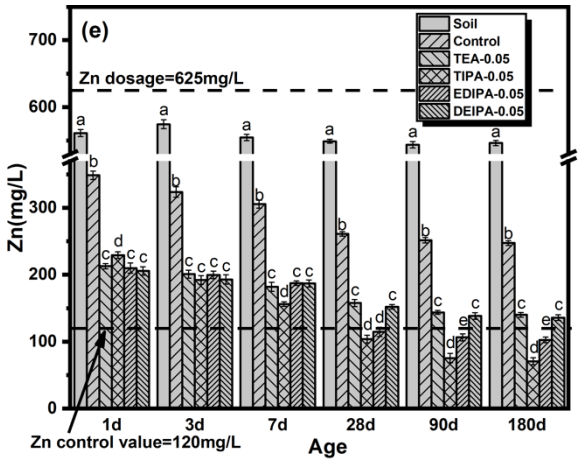

Fig. 10 Effect of different alkanolamines (TEA, TIPA, EDIPA and DEIPA at 0.05% dosage) activated SS on the leachability of HM: (a) Cd, (b) Cu, (c) Ni, (d) Pb and (e) Zn.

3.4.2 Effect of TIPA dosage

According to the above results, TIPA showed the highest effectiveness to solidify and stabilize HM in contaminated soil. Thus, the effect of its dosage on the leachability of HM was investigated with TCLP results shown in Fig. 11. All the HM showed decreased leached concentrations over time. Consistent with the hydration and mechanical results, more TIPA showed improved HM immobilization capacity due to the enhanced hydration of SS. At the dosage > 0.8% the leachability of Ni also dropped to below its regulatory limit at 90 days.

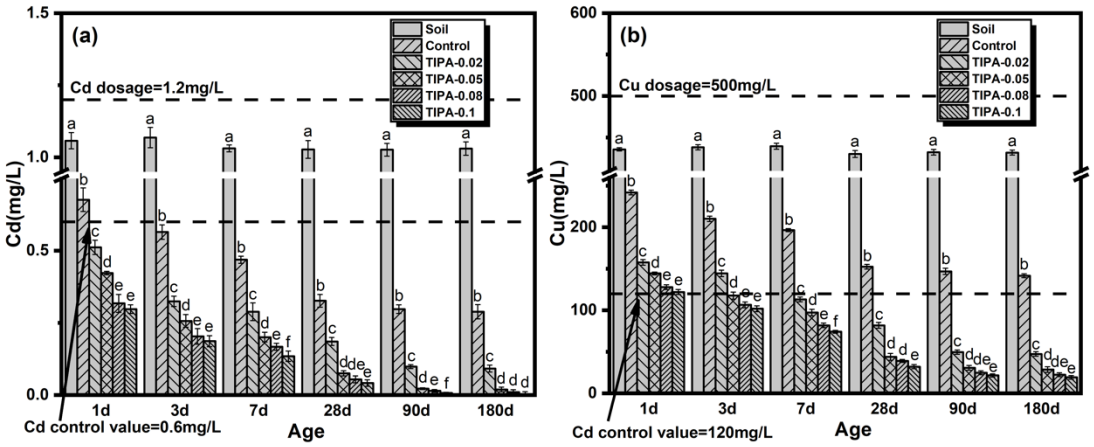

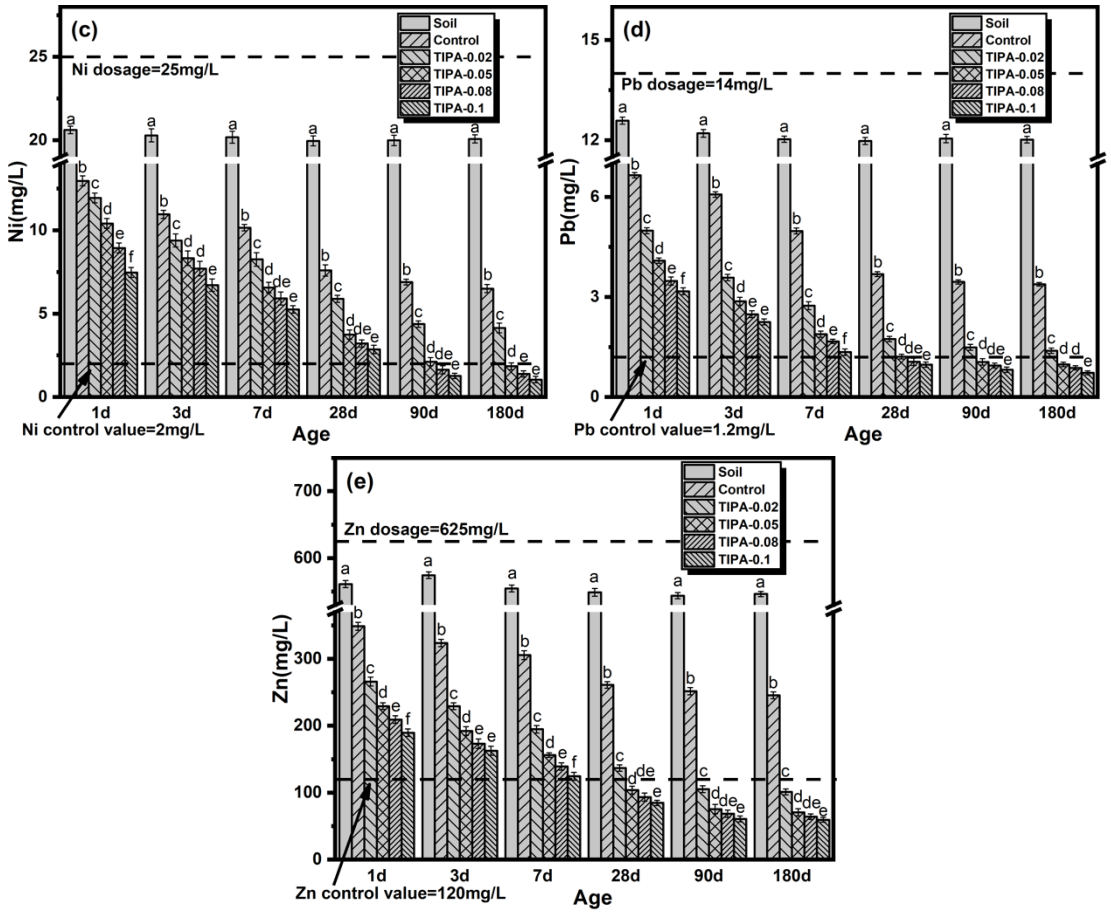

Fig. 11 Effect of dosage of TIPA (0.02%, 0.05%, 0.08% and 0.1%) activated SS on the leachability of HM: (a) Cd, (b) Cu, (c) Ni, (d) Pb and (e) Zn.

4. Discussion

Based on the experimental results presented above, TIPA was found to be the best activator among the four types of alkanolamines, which was studied in detail. Hence the following sections will use TIPA as the representative alkanolamine to elucidate its effect on SS hydration and soil S/S performance.

4.1 Effect on the hydration process

The hydration process of TIPA-activated SS was characterized by the evolution of hydration heat and conductivity over time, and the results agreed well (see Figs. 4 & 5). The hydration process is hence divided into two stages. The first stage is the continuous dissolution of minerals and gradual accumulation of ions in the pore solution. TIPA effectively promotes the dissolution of SS, which was evidenced by the enhancement of the first exothermic peak of hydration heat and the first conductivity peak. This effect is more pronounced with the increased dosage of TIPA. Moreover, the dormant periods between the first and second peak (not observed in the reference SS samples

within the test time) in both the heat and conductivity evolution curves were significantly reduced, indicating the fast accumulation of ions to achieve the supersaturations for hydration products, which induced the second stage. The second stage is the precipitation of hydration products. The enhancement of second peak of hydration heat and the increased difference between the peak and residual conductivity showed that TIPA led to the formation of more hydration products. Similarly, this effect is positively correlated with the dosage of TIPA. This was further evidence by the XRD and TGA results. Hence, the strength of the SS pastes improved remarkably with the increase of TIPA content (Fig. 8).

4.2 Effect on the hydration products

As shown in the XRD and TGA (see Figs. 6 &7), TIPA promoted the dissolution of minerals in SS and the formation of hydration products. This effect is mainly exerted in two ways. The first one is the promotion of the hydration of C_2S, aluminates and C_2F, resulting in the formation of C-S-H, C-A-H and C-F-H. The other way is the enhanced reaction between C-A-H, C-F-H and $CaCO_3$, thereby producing a large amount of Mc.

The mineral phases in SS first dissolve into ions, which accumulate in the cement pore solution (Equations 1-3), and they react with each other to form hydration products. The alkanolamines chelated with the metal ions, which increased the solubility of the minerals and the concentrations of ions [29, 42].

$$2(2CaO \cdot SiO_2) + 4H_2O \rightarrow 3CaO \cdot 2SiO_2 \cdot 3H_2O + Ca^{2+} + 2OH^- \quad (1)$$

$$3CaO \cdot Al_2O_3 + 6H_2O \rightarrow 3Ca^{2+} + 2Al(OH)_4^- + 4OH^- \quad (2)$$

$$2CaO \cdot Fe_2O_3 + H_2O + 2OH^- \rightarrow 2Ca^{2+} + 2Fe(OH)_6^{3-} \quad (3)$$

The ions in the pore solution were chelated by TIPA and would not immediately participate in the precipitation reaction. According to Le Chatelier's principle, the forward progress of reactions (1)-(3) were facilitated until a new value of the dissolution equilibrium constant K was reached [53]. Thus, TIPA promoted the dissolution of mineral phases and increased the amount of various dissolved metal ions in the solution. The precipitation reactions of ions are described in Equations (4) - (8).

$$3Ca^{2+} + 2Al(OH)_4^- + 4OH^- \rightarrow 3CaO \cdot Al_2O_3 \cdot 6H_2O \quad (4)$$

$$3Ca^{2+} + 2Fe(OH)_6^{3-} \rightarrow 3CaO \cdot Fe_2O_3 \cdot 6H_2O \quad (5)$$

$$3Ca^{2+} + 2Al(OH)_4^- + CaCO_3 + 4OH^- + 5H_2O \rightarrow 3CaO \cdot Al_2O_3 \cdot CaCO_3 \cdot 11H_2O \quad (6)$$

$$3Ca^{2+} + 2Fe(OH)_6^{3-} + CaCO_3 + 5H_2O \rightarrow 3CaO \cdot Fe_2O_3 \cdot CaCO_3 \cdot 11H_2O \quad (7)$$

$$4Ca^{2+} + (2x)Al(OH)_4^- + [2(1\text{-}x)]\, Fe(OH)_6^{3-} + CO_3^{2-} + 4xOH^- + 5H_2O$$

$$\rightarrow 3CaO \cdot xAl_2O_3 \cdot (1-x)Fe_2O_3 \cdot CaCO_3 \cdot 11H_2O \quad (8)$$

The precipitation led to the reduction of metal ion concentrations in the pore solution, resulting in the release of ions from their chelated forms, further promoting the precipitation of more hydration products. The dissolution and precipitation reactions are hence both promoted by TIPA which acts like a "catalyst" in the process. In summary, TIPA promoted the dissolution of mineral phases such as C_2S, C_3A, $C_{12}A_7$, and C_2F, thereby increased the amount of metal ions in the solution, and hence promoted the subsequent precipitation reaction of generating C-S-H, C-A-H, C-F-H and Mc. Nevertheless, how different alkanolamines interacted with the ions and affected the hydration of SS differently remain unclear.

4.3 Effect on the S/S performance for HM-contaminated soil

TIPA-activated SS showed excellent compatibility with the heavily contaminated soil, which was evidenced by the UCS of the mixtures (see Fig.9). Moreover, the leachability of all HM (except for Ni) can be successfully reduced to below their regulatory limits with only 0.5% of TIPA in SS at the curing age of 28 days, while Ni was successfully treated at 90 days with 0.8% TIPA-activated SS. The outstanding S/S performance is partly due to the enhanced solidification due to better cementitious properties of TIPA-activated SS and also due to the enhanced chemical stabilisation of HM in the hydration products such as C-S-H, C-A-H, C-F-H and Mc [54-56]. Moreover, TIPA may also play a role in stabilizing HM by chelation, which warrant further studies. Leaching effect of HM in the hydration products of alkanolamines activated SS was shown in Fig. S1 and Fig. S2. The leaching of each heavy metal remained relatively constant after the age of 28d, which demonstrates that the solidification and stabilization of heavy metals by SS hydration products is firm and stable. This study demonstrated that alkanolamines could improve the capacity of SS to solidify and stabilize HM-contaminated soil. Firstly, it provides a sustainable alternative to Portland cement in S/S to reduce energy consumption and carbon emission in cement production. Secondly, it will

enhance the utilization of SS to reduce the environmental impact and waste of land resources. However, there are many challenges and opportunities to apply this novel binder in the field which include but not limited to: (i) optimisation of the alkanolamines/SS and SS/soil ratios depending on the type, concentration of the contaminants and the soil type; (ii) long-term performance of the treated soils under different climatic conditions; and (iii) variability of the SS composition in the world and hence the potential of leaching inherent contaminants in SS in the long term.

5. Conclusion

Four types of alkanolamines (TEA, TIPA, EDIPA and DEIPA) were used to activate SS and then remediate HM-contaminated soil. The effects of alkanolamines on the hydration process and hydration products of SS were thoroughly investigated via a series of techniques. Moreover, their effects on the stabilization/solidification performance of HM-contaminated soil were assessed via strength and leaching tests. The following conclusions could be drawn:

1. The addition of alkanolamines promoted the hydration process of SS and hence facilitated the formation of hydration products. The chelation of dissolved metal ions promoted the dissolution of mineral phases in SS and the subsequent precipitation reaction. The hydration products such as C-S-H, C-A-H, C-F-H and Mc were beneficial to solidify and stabilize heavy metal contaminated soil.

2. TIPA showed the best activation effect among all the investigated alkanolamines and better promotion effect could be obtained with higher dosage. Compared to the reference SS paste, the compressive strength of the 0.1% TIPA-activated SS was enhanced by 190.5% at 28 days.

3. TIPA-activated SS showed excellent performance in HM-contaminated soil stabilization/solidification. Leached concentrations of Cd, Cu, Ni, Pb, and Zn have reduced by 87.2%, 78.8%, 62.4%, 73.6% and 64.5% using 0.1% TIPA-activated SS after 28 days, and they were all below their respective regulatory limits by Standard for Pollution Control on the Hazardous Waste Landfill (GB 18598-2019) in China. Compared to the reference SS, the UCS of the treated soil at 28 days was enhanced by 237.7% using 0.1% TIPA-activated SS.

This study proposed a promising way of upcycling SS as a soil remediation agent to promote circular economy, which would not only alleviate the environmental problems of disposing SS but also provide a sustainable alternative to Portland cement in stabilization/solidification, contributing to a low-carbon future.

Declaration of Competing Interest

We declare that we do not have any commercial or associative interest that represents a conflict of interest in connection with the work submitted.

Acknowledgments

We are grateful to the financial supports by State Key Laboratory of Materials-Oriented Chemical Engineering (No.SKL-MCE-22A07), National Natural Science Foundation of China (52272018), National Key R&D Program of China (2021YFB3802002), a Project Funded by the Priority Academic Program Development (PAPD) of Jiangsu Higher Education Institutions.

References

[1] B. Zeng, Q. Wang, L. Mo, F. Jin, J. Zhu, M. Tang, Synthesis of Mg-Al LDH and its calcined form with natural materials for efficient Cr(VI) removal, Journal of Environmental Chemical Engineering, 10 (2022).

[2] M.-K. Zhang, Z.-Y. Liu, H. Wang, Use of Single Extraction Methods to Predict Bioavailability of Heavy Metals in Polluted Soils to Rice, Communications in Soil Science and Plant Analysis, 41 (2010) 820-831.

[3] Y.-L. Yang, K.R. Reddy, Y.-J. Du, R.-D. Fan, Sodium hexametaphosphate (SHMP)-amended calcium bentonite for slurry trench cutoff walls: workability and microstructure characteristics, Canadian Geotechnical Journal, 55 (2018) 528-537.

[4] Y. Yang, Reddy, KR, Du, YJ, Fan, RD, Short-Term Hydraulic Conductivity and Consolidation Properties of Soil-Bentonite Backfills Exposed to CCR-Impacted Groundwater., JOURNAL OF GEOTECHNICAL AND GEOENVIRONMENTAL ENGINEERING, 144 (2018).

[5] D. Hou, F. Li, Complexities Surrounding China's Soil Action Plan, Land Degradation & Development, 28 (2017) 2315-2320.

[6] Y. Song, N. Kirkwood, C. Maksimovic, X. Zheng, D. O'Connor, Y. Jin, D. Hou, Nature based solutions for contaminated land remediation and brownfield redevelopment in cities: A review, Sci Total Environ, 663 (2019) 568-579.

[7] C. Qu, W. Shi, J. Guo, B. Fang, S. Wang, J.P. Giesy, P.E. Holm, China's Soil Pollution Control: Choices and Challenges, Environmental science & technology, 50 (2016) 13181-13183.

[8] Z. Shen, D. Hou, B. Zhao, W. Xu, Y.S. Ok, N.S. Bolan, D.S. Alessi, Stability of heavy metals in soil washing residue with and without biochar addition under accelerated ageing, Sci Total Environ, 619-620 (2018) 185-193.

[9] Y.J. Du, M.L. Wei, K.R. Reddy, Z.P. Liu, F. Jin, Effect of acid rain pH on leaching behavior of cement stabilized lead-contaminated soil, J Hazard Mater, 271 (2014) 131-140.

[10] D. Hou, A. Al-Tabbaa, D. O'Connor, Q. Hu, Y.-G. Zhu, L. Wang, N. Kirkwood, Y.S. Ok, D.C.W. Tsang, N.S. Bolan, J. Rinklebe, Sustainable remediation and redevelopment of brownfield sites, Nature Reviews Earth & Environment, (2023).

[11] D. Hou, Q. Gu, F. Ma, S. O'Connell, Life cycle assessment comparison of thermal desorption and stabilization/solidification of mercury contaminated soil on agricultural land, Journal of Cleaner Production, 139 (2016) 949-956.
[12] J.R. Conner, S.L. Hoeffner, The History of Stabilization/Solidification Technology, Critical Reviews in Environmental Science and Technology, 28 (1998) 325-396.
[13] Z. Shen, F. Jin, D. O'Connor, D. Hou, Solidification/Stabilization for Soil Remediation: An Old Technology with New Vitality, Environ Sci Technol, 53 (2019) 11615-11617.
[14] F. Wang, F. Jin, Z. Shen, A. Al-Tabbaa, Three-year performance of in-situ mass stabilised contaminated site soils using MgO-bearing binders, J Hazard Mater, 318 (2016) 302-307.
[15] J. Shu, R. Liu, Z. Liu, H. Chen, J. Du, C. Tao, Solidification/stabilization of electrolytic manganese residue using phosphate resource and low-grade MgO/CaO, J Hazard Mater, 317 (2016) 267-274.
[16] F. Jin, Long-term effectiveness of in situ solidification/stabilization, in: Sustainable Remediation of Contaminated Soil and Groundwater, 2020, pp. 247-278.
[17] A.A.V. Cerbo, F. Ballesteros, T.C. Chen, M.-C. Lu, Solidification/stabilization of fly ash from city refuse incinerator facility and heavy metal sludge with cement additives, Environmental Science and Pollution Research, 24 (2016) 1748-1756.
[18] Z. Shen, S. Pan, D. Hou, D. O'Connor, F. Jin, L. Mo, D. Xu, Z. Zhang, D.S. Alessi, Temporal effect of MgO reactivity on the stabilization of lead contaminated soil, Environment international, 131 (2019) 104990.
[19] Y.-S. Wang, J.-G. Dai, L. Wang, D.C.W. Tsang, C.S. Poon, Influence of lead on stabilization/solidification by ordinary Portland cement and magnesium phosphate cement, Chemosphere, 190 (2018) 90-96.
[20] K.L. Scrivener, R.J. Kirkpatrick, Innovation in use and research on cementitious material, Cement and Concrete Research, 38 (2008) 128-136.
[21] Z. Shen, D. Hou, W. Xu, J. Zhang, F. Jin, B. Zhao, S. Pan, T. Peng, D.S. Alessi, Assessing long-term stability of cadmium and lead in a soil washing residue amended with MgO-based binders using quantitative accelerated ageing, Sci Total Environ, 643 (2018) 1571-1578.
[22] F. Wang, H. Wang, A. Al-Tabbaa, Leachability and heavy metal speciation of 17-year old stabilised/solidified contaminated site soils, J Hazard Mater, 278 (2014) 144-151.
[23] M.L. Wei, Y.J. Du, K.R. Reddy, H.L. Wu, Effects of freeze-thaw on characteristics of new KMP binder stabilized Zn- and Pb-contaminated soils, Environ Sci Pollut Res Int, 22 (2015) 19473-19484.
[24] Y.J. Du, N.J. Jiang, S.L. Shen, F. Jin, Experimental investigation of influence of acid rain on leaching and hydraulic characteristics of cement-based solidified/stabilized lead contaminated clay, J Hazard Mater, 225-226 (2012) 195-201.
[25] Y.-J. Du, N.-J. Jiang, S.-Y. Liu, F. Jin, D.N. Singh, A.J. Puppala, Engineering properties and microstructural characteristics of cement-stabilized zinc-contaminated kaolin, Canadian Geotechnical Journal, 51 (2014) 289-302.
[26] P. Liu, J. Zhong, M. Zhang, L. Mo, M. Deng, Effect of CO2 treatment on the microstructure and properties of steel slag supplementary cementitous materials, Construction and Building Materials, 309 (2021).
[27] F. Han, Z. Zhang, D. Wang, P. Yan, Hydration heat evolution and kinetics of blended cement containing steel slag at different temperatures, Thermochimica Acta, 605 (2015) 43-51.
[28] B. Pang, Z. Zhou, H. Xu, Utilization of carbonated and granulated steel slag aggregate in concrete, Construction and Building Materials, 84 (2015) 454-467.

[29] S. Yang, J. Wang, S. Cui, H. Liu, X. Wang, Impact of four kinds of alkanolamines on hydration of steel slag-blended cementitious materials, Construction and Building Materials, 131 (2017) 655-666.
[30] L. Mo, S. Yang, B. Huang, L. Xu, S. Feng, M. Deng, Preparation, microstructure and property of carbonated artificial steel slag aggregate used in concrete, Cement and Concrete Composites, 113 (2020).
[31] S. Yang, L. Mo, M. Deng, Effects of ethylenediamine tetra-acetic acid (EDTA) on the accelerated carbonation and properties of artificial steel slag aggregates, Cement and Concrete Composites, 118 (2021).
[32] J. Sun, Z. Zhang, S. Zhuang, W. He, Hydration properties and microstructure characteristics of alkali–activated steel slag, Construction and Building Materials, 241 (2020).
[33] R. Cao, Z. Jia, Z. Zhang, Y. Zhang, N. Banthia, Leaching kinetics and reactivity evaluation of ferronickel slag in alkaline conditions, Cement and Concrete Research, 137 (2020).
[34] Q. Wang, P. Yan, J. Yang, B. Zhang, Influence of steel slag on mechanical properties and durability of concrete, Construction and Building Materials, 47 (2013) 1414-1420.
[35] N.K. Lee, J.G. Jang, H.K. Lee, Shrinkage characteristics of alkali-activated fly ash/slag paste and mortar at early ages, Cement and Concrete Composites, 53 (2014) 239-248.
[36] E. Adesanya, K. Ohenoja, A. Di Maria, P. Kinnunen, M. Illikainen, Alternative alkali-activator from steel-making waste for one-part alkali-activated slag, Journal of Cleaner Production, 274 (2020).
[37] Y. Zhou, J. Sun, Y. Liao, Influence of ground granulated blast furnace slag on the early hydration and microstructure of alkali-activated converter steel slag binder, Journal of Thermal Analysis and Calorimetry, 147 (2020) 243-252.
[38] W. Li, S. Ma, Y. Hu, X. Shen, The mechanochemical process and properties of Portland cement with the addition of new alkanolamines, Powder Technology, 286 (2015) 750-756.
[39] Z. Xu, W. Li, J. Sun, Y. Hu, K. Xu, S. Ma, X. Shen, Research on cement hydration and hardening with different alkanolamines, Construction and Building Materials, 141 (2017) 296-306.
[40] Z. Yan-Rong, K. Xiang-Ming, L. Zi-Chen, L. Zhen-Bao, Z. Qing, D. Bi-Qin, X. Feng, Influence of triethanolamine on the hydration product of portlandite in cement paste and the mechanism, Cement and Concrete Research, 87 (2016) 64-76.
[41] L. Chang, H. Liu, J. Wang, H. Liu, L. Song, Y. Wang, S. Cui, Effect of chelation via ethanol-diisopropanolamine on hydration of pure steel slag, Construction and Building Materials, 357 (2022).
[42] J. Wang, L. Chang, D. Yue, Y. Zhou, H. Liu, Y. Wang, S. Yang, S. Cui, Effect of chelating solubilization via different alkanolamines on the dissolution properties of steel slag, Journal of Cleaner Production, 365 (2022).
[43] J.E.-. Research institute of highway ministry of transport, Test methods of materials stabilized with inorganic binders of highway engineering, Beijing: China Communications Press, (2009).
[44] C. Hesse, F. Goetz-Neunhoeffer, J. Neubauer, A new approach in quantitative in-situ XRD of cement pastes: Correlation of heat flow curves with early hydration reactions, Cement and Concrete Research, 41 (2011) 123-128.
[45] D. Jansen, F. Goetz-Neunhoeffer, B. Lothenbach, J. Neubauer, The early hydration of Ordinary Portland Cement (OPC): An approach comparing measured heat flow with calculated heat flow from QXRD, Cement and Concrete Research, 42 (2012) 134-138.
[46] S. Ma, W. Li, S. Zhang, Y. Hu, X. Shen, Study on the hydration and microstructure of Portland cement containing diethanol-isopropanolamine, Cement and Concrete Research, 67 (2015) 122-130.
[47] B. Huo, B. Li, C. Chen, Y. Zhang, Surface etching and early age hydration mechanisms of steel slag

powder with formic acid, Construction and Building Materials, 280 (2021).
[48] H. Tan, Y. Guo, F. Zou, S. Jian, B. Ma, Z. Zhi, Effect of borax on rheology of calcium sulphoaluminate cement paste in the presence of polycarboxylate superplasticizer, Construction and Building Materials, 139 (2017) 277-285.
[49] Q. Wang, P. Yan, Hydration properties of basic oxygen furnace steel slag, Construction and Building Materials, 24 (2010) 1134-1140.
[50] Z. Chen, K. Tu, R. Li, J. Liu, Study on the application mechanism and mechanics of steel slag in composite cementitious materials, SN Applied Sciences, 2 (2020).
[51] D. Wang, J. Chang, W.S. Ansari, The effects of carbonation and hydration on the mineralogy and microstructure of basic oxygen furnace slag products, Journal of CO_2 Utilization, 34 (2019) 87-98.
[52] China, Standard for pollution control on the hazardous waste landfill, GB 18598-2019
[53] I. Novak, Geometrical Description of Chemical Equilibrium and Le Châtelier's Principle: Two-Component Systems, Journal of Chemical Education, 95 (2017) 84-87.
[54] Q. Wang, M. Li, J. Yang, J. Cui, W. Zhou, X. Guo, Study on mechanical and permeability characteristics of nickel-copper-contaminated soil solidified by CFG, Environ Sci Pollut Res Int, 27 (2020) 18577-18591.
[55] W. Li, P. Ni, Y. Yi, Comparison of reactive magnesia, quick lime, and ordinary Portland cement for stabilization/solidification of heavy metal-contaminated soils, Sci Total Environ, 671 (2019) 741-753.
[56] L. Sha, Z. Zou, J. Qu, X. Li, Y. Huang, C. Wu, Z. Xu, As(III) removal from aqueous solution by katoite (Ca(3)Al(2)(OH)(12)), Chemosphere, 260 (2020) 127555.